



## Nanomaterial-Based Repurposing of Macrophage Metabolism and Its Applications

### Cite as

Nano-Micro Lett.

(2024) 16:246

Tingting Meng<sup>1</sup>, Danfeng He<sup>1</sup>, Zhuolei Han<sup>1</sup>, Rong Shi<sup>1,2</sup>, Yuhan Wang<sup>1</sup>, Bibo Ren<sup>1</sup>, Cheng Zhang<sup>1</sup>, Zhengwei Mao<sup>1,3</sup> ✉, Gaoxing Luo<sup>1</sup> ✉, Jun Den<sup>1</sup> ✉

Received: 7 March 2024

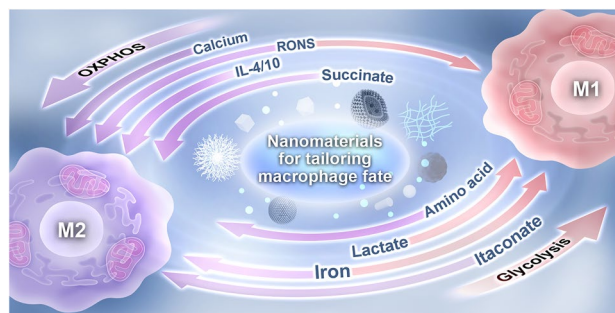
Accepted: 10 June 2024

© The Author(s) 2024

### HIGHLIGHTS

- A large-scale metabolic adaptation in M1-polarized macrophages compared with M2 macrophages, along with multiple altered metabolite parameters that can serve as potential targets, have been discussed.
- Nanomaterial-based repurposing of macrophage metabolism and its applications are systematically summarized and illustrated using representative examples.
- Potential challenges, additional information about future research objectives, and priorities of nanomaterial-based macrophage immunotherapy are highlighted.

**ABSTRACT** Macrophage immunotherapy represents an emerging therapeutic approach aimed at modulating the immune response to alleviate disease symptoms. Nanomaterials (NMs) have been engineered to monitor macrophage metabolism, enabling the evaluation of disease progression and the replication of intricate physiological signal patterns. They achieve this either directly or by delivering regulatory signals, thereby mapping phenotype to effector functions through metabolic repurposing to customize macrophage fate for therapy. However, a comprehensive summary regarding NM-mediated macrophage visualization and coordinated metabolic rewiring to maintain phenotypic equilibrium is currently lacking. This review aims to address this gap by outlining recent advancements in NM-based metabolic immunotherapy. We initially explore the relationship between metabolism, polarization, and disease, before delving into recent NM innovations that visualize macrophage activity to elucidate disease onset and fine-tune its fate through metabolic remodeling for macrophage-centered immunotherapy. Finally, we discuss the prospects and challenges of NM-mediated metabolic immunotherapy, aiming to accelerate clinical translation. We anticipate that this review will serve as a valuable reference for researchers seeking to leverage novel metabolic intervention-matched immunomodulators in macrophages or other fields of immune engineering.



**KEYWORDS** Immunomodulatory nanomaterial; Macrophage polarization; Macrophage metabolic reprogramming; Immune engineering

Tingting Meng, Danfeng He and Zhuolei Han have contributed equally to this work.

✉ Zhengwei Mao, [zwmao@zju.edu.cn](mailto:zwmao@zju.edu.cn); Gaoxing Luo, [logxw@hotmail.com](mailto:logxw@hotmail.com); Jun Den, [djun.123@163.com](mailto:djun.123@163.com)

<sup>1</sup> Institute of Burn Research, Southwest Hospital, State Key Laboratory of Trauma and Chemical Poisoning, Army Medical University, Chongqing 400038, People's Republic of China

<sup>2</sup> Department of Breast Surgery, Gansu Provincial Hospital, Lanzhou, Gansu 730030, People's Republic of China

<sup>3</sup> MOE Key Laboratory of Macromolecular Synthesis and Functionalization, Department of Polymer Science and Engineering, Zhejiang University, Hangzhou 310027, People's Republic of China

Published online: 15 July 2024



SHANGHAI JIAO TONG UNIVERSITY PRESS

Springer

## 1 Introduction

Macrophages are vital cellular components of the innate immune system, playing crucial roles in regulating inflammatory responses to maintain tissue homeostasis [1–3]. However, macrophage responses represent a double-edged sword, acting both as a protective “safety guard” and as a potential instigator of disease [4]. They exhibit a full spectrum of polarized phenotypes, encompassing proinflammatory-like (M1) and anti-inflammatory-like (M2) states [5–9] (Table 1). Macrophage polarization (M1/M2) remains dynamic and finely balanced due to their heterogeneity and plasticity, adapting to tailored cues in the physiological microenvironment [9, 10].

Immunometabolism has provided novel insights into the hyperactivation of macrophage metabolism. M1 macrophages rewrite their metabolic program to coordinate the adaptive immune response compared to M2 macrophages, which rely on oxidative phosphorylation (OXPHOS). The metabolic adaption includes an interrupted tricarboxylic acid (TCA) cycle, increased activation of glycolysis and the pentose phosphate pathway (PPP), and alterations in various metabolic parameters such as succinate or itaconate, reactive oxygen and nitrogen species (RONS), and amino acids [11–15]. Several excellent reviews have elaborately described the intricate relationship between macrophage polarization and metabolism [11, 13, 14, 16]. This alteration-coordinated metabolic rewiring profoundly influences macrophage gene expression, leading to unbalanced M1/M2 polarization [16–19], which determines the progression of diseases such as osteoarthritis (OA) [20], acute lung injury (ALI) [21], myocardial infarction (MI) [22], diabetic wounds [23, 24], atherosclerosis [25], and inflammatory bowel disease (IBD) [26]. Conversely,

tumor-associated macrophages (TAMs) initially exhibit a higher glycolysis rate to support antitumor M1 activity, but gradually transition toward more efficient OXPHOS and fatty acid oxidation (FAO) to promote protumor M2 functions, thereby facilitating tumor immune escape [18, 27–30]. Given the critical role of altered metabolic profiles as positive or negative regulators of macrophage fate in driving disease evolution, in situ tracking of macrophage metabolism holds significant importance for elucidating disease progression. Moreover, intervening in metabolism to exacerbate metabolic imbalance or restore metabolic homeostasis has been exploited as a fascinating avenue to reshape macrophage phenotypes and elicit the corresponding immune response against diseases.

Nanomaterials (NMs) have been extensively fabricated to display and transmit macrophage regulatory signals in a precise and closely physiological manner, simulating artificial microenvironments and guiding macrophage fate [31]. This is benefited by their intrinsic physicochemical properties and macrophage phagocytosis, in which foreign particles are preferentially internalized [32, 33]. Recently, the metabolic pathways of M1/M2 macrophages have garnered increasing attention from researchers, leading to their adoption in macrophage diagnosis and therapeutic exploitation. This trend has facilitated the blossom of suitable theranostic agents for macrophage-driven diseases. Several researchers have exploited imaging probes, integrating them with advanced technologies such as magnetic resonance imaging (MRI), to track macrophage activity in situ and reveal disease progression [34–38], such as dual-responsive nanoreporters for monitoring macrophage phenotypes [39]. NMs serve as emerging immunomodulatory weapons, enabling the remote manipulation of macrophage metabolism [19, 31, 40], thereby directing their

**Table 1** Potential metabolic targets of macrophages and M1/M2-like biomarkers

Metabolic targets	M1 biomarkers	M2 biomarkers
(1) RONS	(1) Activated inducer: LPS, IFN- $\gamma$	(1) Activated inducer: IL-4, IL-13
Itaconate	(2) Surface marker: CD80, CD86, CD68, TLR-2/4	(2) Surface marker: CD163, CD206
Iron	(3) Secreted cytokines: TNF- $\alpha$ , IL-1 $\beta$ , IL-6/12/23/17A, IFN- $\beta$	(3) Secreted cytokines: IL-10, TGF- $\beta$ , VEGF $\alpha$ , bFGF
IL-4	(4) Secreted chemokines: CCL-2/9/11, CXCL-2, CCR7	(4) Secreted chemokines: CCL-1/17/
IL-10	(5) Marker gene: <i>NOS2</i> , <i>Nfkbiz</i> , <i>IFN-<math>\alpha</math></i> , <i>S100a9a</i> , <i>IFN-<math>\alpha/\beta</math></i> , <i>Edn-</i> , <i>Irf-5</i>	(5) Marker gene: <i>Arg-1</i> , <i>Fizz-1</i> , <i>Ym-1</i> , <i>KLF-4</i> , <i>Smad3</i>
Calcium	(6) Signaling molecule: iNOS, Socs-3, STAT-1	(6) Signaling molecule: STAT6, Arg-1
Amino acid		(7) Receptor: MerTK, TLR1/8
Lactate		

polarization toward desired phenotypes for disease therapy [41], such as nanozymes combating inflammatory diseases by ROS scavenging-primed M2-like [42, 43]. However, there remains a lack of in-depth summary and discussion regarding current strategies for tracing metabolic signatures to elucidate diseases and subsequently reorienting macrophage fate for immunotherapy targeting macrophage-centered diseases.

Here, we review recent advances in NM-mediated macrophage immunotherapy from a metabolic perspective (Fig. 1 and Table 2). We first provide a comprehensive overview of differentiated metabolism in polarized macrophages, followed by the relationship between metabolism and disease. Next, we systematically summarize the visualization of macrophage behavior in situ using NMs to reveal disease progression, as well as NM-mediated metabolic rewiring to re-educate macrophage fate for disease therapy. This review could serve as a versatile toolbox for researchers in various fields. Finally, we discuss the challenges and future research directions in exploiting NMs to reprogram macrophage metabolism. We anticipate that this review will contribute to advancing the understanding of research progress in regenerative medicine materials mounted on macrophage immune responses by modulating metabolism, guiding the reasonable design of immunomodulatory biomaterials to re-educate macrophage responses, and driving the application of macrophage immunotherapy in the field of immune engineering.

## 2 Macrophage Metabolism: An Underlying Target for Tailoring Macrophage-Centered Diseases

The metabolic reprogramming of macrophages is strongly associated with their polarization [44–46] (Fig. 2). Macrophages coordinate their own response to oxygen gradient [8]. Contrary to M2, which have an intact TCA cycle that maintains a sustained supply of ATP (~30 per glucose) through OXPHOS and FAO to improve tissue repair, M1 macrophages substantially undergo enhanced glycolytic metabolism and impaired OXPHOS to adapt to hypoxia. Glycolysis produces less ATP (~2 per glucose) at a faster rate than OXPHOS and provides metabolic intermediates required for the biosynthesis of nucleotides, amino acids, and fatty acids [47].

LPS(+ IFN- $\gamma$ )-activated M1 macrophages upregulate glucose transporter-1 (Glut1) to enhance glucose uptake [48] and upregulate glycolytically rate-limiting enzymes such as pyruvate kinase M2 (PKM2) to activate the glycolytic pathway. This pathway generates pyruvate to fuel the TCA cycle and produces lactate by lactate dehydrogenase (LDH)-catabolized pyruvate [49]. PKM2 enhances IL-6 and IL-1 $\beta$  secretion by phosphorylating signal transducer and activator of transcription (STAT) 3 and induces inflammasome-mediated pro-IL-1 $\beta$  and IL-1 $\beta$  secretion through HIF-1 $\alpha$  activity [50, 51]. Moreover, NADPH derived from upregulated PPP in M1 macrophage overproduced ROS via NADPH oxidase [24, 52].

Two metabolic breakpoints occur in the truncated TCA cycle of M1-polarized macrophages [14, 15, 53]. The first breakpoint occurs at the downregulated isocitrate dehydrogenase (IDH) 1, which converts isocitrate into  $\alpha$ -ketoglutarate ( $\alpha$ -KG) in M2, resulting in citrate accumulation, facilitating the biosynthesis of fatty acids and prostaglandins in M1 macrophages [12]. Glutamine enters the cytosol via the ASCT2/SN2 transporter and is metabolized to glutamate via glutaminase, followed by forming  $\alpha$ -KG to fuel the TCA cycle occurred at interrupted  $\alpha$ -KG production caused by IDH1 silence, and is termed glutamine anaplerosis [54]. The accumulated citrate is metabolized by citrate lyase into oxaloacetic acid and acetyl-CoA (precursors for ROS and NO, respectively) after transport to the cytosol via citric acid transporter [14, 15]. Intriguingly, immune-responsive gene 1 (IRG1) redirects citrate to itaconate, which synergizes with NO to block succinate dehydrogenase (SDH), forming the second breakpoint, which accumulates inflammatory succinate [14]. The succinate receptor, G protein-coupled receptor-9 (GPR91), recognizes extracellular succinate from M1 macrophages to form a feedforward loop to induce macrophage activation [55, 56].

The broken TCA cycle is co-opted to form an aspartate–argininosuccinate shunt (AASS) that feeds the TCA cycle at fumarate and replenishes the cycle after the breakpoint at SDH. AASS links the TCA cycle to the urea cycle, a metabolic pathway closely involved in NO production [13, 15, 16]. Intriguingly, blocking the rate-limiting enzyme of AASS, aspartate arginine succinate shunt enzyme, inhibits NO/IL-6 production and inducible nitric oxide synthase (iNOS) expression, both of which are biomarkers for M1 [5].

Amino acids feed the TCA cycle and compensate the level of intermediates in this pathway [13, 16]. Arginine is catabolized via the iNOS/Arg-1 axis. In M1 macrophages,

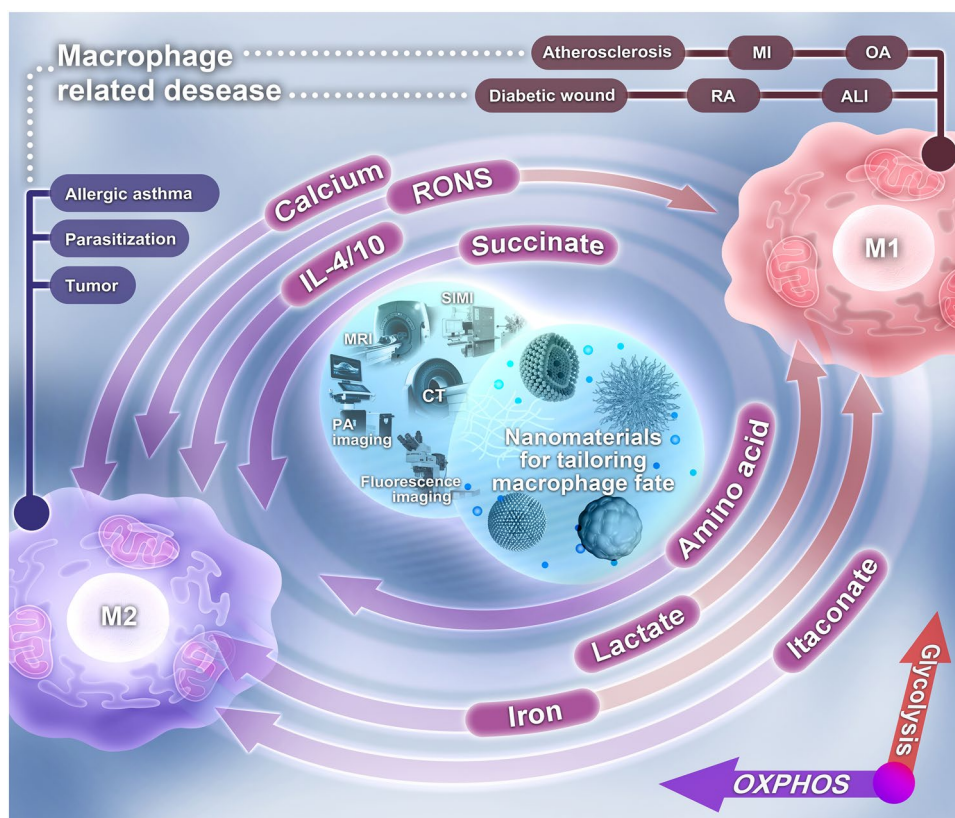


**Fig. 1** A systematic illustration of NM-based repurposing of macrophage metabolism and its applications

upregulated iNOS metabolizes arginine to citrulline and NO [45, 57]. Recycled citrulline synergizes with aspartate to synthesize arginine for NOS reuse in turn by upregulating argininosuccinate synthase and argininosuccinate lyase in M1 macrophages through the citrulline–NO cycle [58]. The initial NO burst in M1 derives from extracellular arginine [59]. Multiple pathways-produced NO nitrosylates iron–sulfur-containing proteins to inhibit the electron transport chain (complexes I, II, and IV), thereby impairing OXPHOS action (e.g., electron transport, ATP production) against bacteria and tumor or causing other diseases [60, 61]. Repurposing mitochondria to produce mitochondrial ROS (mtROS) is an outcome of impaired OXPHOS [62]. Conversely, elevated Arg-1 in M2 competes with the iNOS-arginine pathway and hydrolyzes arginine to polyamines, supporting tissue remodeling [58, 63]. Polyamine production initiates M2 polarization [64].

Macrophages regulate iron metabolism. Physiological iron uptake primarily relies on heme oxygenase (HO)-mediated iron recycling, predominantly stores in labile iron pool (LIP) by binding ferritin (Ft), and releases iron through transferrin

receptor 1 [65]. Ferroportin (FPN)-excreted free iron avoids oxidative damage caused by iron-induced Fenton reaction [66, 67]. Iron metabolism defines macrophage subsets, with M1 macrophages increasing iron retention to exhibit an iron-sequestering phenotype by upregulating ferritin and hepcidin and downregulating TfR1, FPN, and HO-1 expression, compared to M2 macrophages, which exhibit reduced iron levels (termed the iron-releasing phenotype) [68–70]. Iron deprivation in human macrophages directly blocks the transcription of respiratory chain enzymes, such as Fe–S clusters, and increases glucose-derived citrate pools related to lipid accumulation, impairing OXPHOS and increasing glycolytic flux to activate the M1 phenotype. Iron overload promotes ROS production and deviates glycolysis to activate the M1 response. Acute iron chelation in LPS-activated macrophages increases the itaconate/succinate ratio to decrease IL-1 $\beta$  and TNF- $\alpha$  secretion, thus blocking M1 polarization [71].

Calcium homeostasis determines macrophage phenotypes. Excess Ca<sup>2+</sup> stimulates the M1 response. Cytosolic Ca<sup>2+</sup> concentration ([Ca<sup>2+</sup>]<sub>c</sub>) is maintained 1000 times lower than the extracellular level through several Ca<sup>2+</sup> outflow-mediated

**Table 2** NMs repurpose cell metabolism to reorient macrophage fate and their applications

Disease types	Polarized direction	Targets and strategies	Potentially polarized mechanism	Application	References
M1-related	M1-to-M2	RONS, Scavenging RONS	HA@RH-CeO <sub>x</sub> scavenges ROS and inhibits TLR4 signaling pathway	RA	[159]
			MFC-MSNs produce O <sub>2</sub> and scavenge ROS	RA	[155]
			HTON produces H <sub>2</sub> to mediate ROS scavenging	RA	[163]
			PNSG scavenges NO and evokes H <sub>2</sub> S with ROS scavenging ability	RA	[171]
			NAHA-CaP/siRNA releases NO scavenger to eliminate NO and CA9siRNA to silence CA9 expression	OA	[172]
			CAT&SMT@ZIF-8 inhibits NOS activity and catalyzes O <sub>2</sub> production	OA	[173]
			NOArg-PEA reduces NO by re-equilibrating NOS metabolic pathways	Diabetic wound	[174]
			DEX@PPNP scavenges excess ROS/NO and releases DEX to block inflammatory signals	OA	[175]
			DS/TPP-MMSP releases MnO <sub>2</sub> to eliminate ROS and SMT to inhibit NOS for NO production	OA	[20]
			Succinate, Inhibiting SDH	Disodium malonate inhibits SDH activity to block mtROS production	Reperfusion injury
		Itaconate, Supplying itaconate or derivatives		ITA-OD/HD/DD releases ITA to exert anti-inflammatory abilities	Inflammatory diseases
			PCL/DMI also releases DMI to suppress IL-23/17 axis and promote Nrf-2	MI	[178]
		Iron, Depleting iron	P1-3 with DFO and catechol units chelate iron and scavenge iron-induced ROS	ICH	[179]
			P(MMD-co-LA)/DFO captures iron to inhibit ROS formation	Nerve regeneration	[180]
		IL-4, Supplying IL-4	MGC/IL-4 pDNA scavenges ROS and delivers IL-4 pDNA	MI	[181]
			PM-MG-CPIL4 releases IL-4 to initiate IL-4 signaling pathway	Ischemic stroke	[182]
		IL-10, Supplying IL-10	PF-IL-10 releases IL-10	Skin regeneration	[183]
			IL-10 <sup>+</sup> EVs release IL-10 to inhibit mTOR signaling	AKI	[184]
		Calcium, Depleting Ca <sup>2+</sup>	UCNP@mSiO <sub>2</sub> releases Ca <sup>2+</sup> regulators to supply or deplete [Ca <sup>2+</sup> ] <sub>i</sub>	Immune diseases	[185]
			PPTB NPs release BAPTA-AM to glut excess [Ca <sup>2+</sup> ] <sub>m</sub> to reduce mtROS production	Periodontitis	[75]
METP NPs release EGTA to block Ca <sup>2+</sup> influx and inhibit HIF-1 $\alpha$ /ROS production	OA therapy		[186]		
BCP/MVS triggers [Ca <sup>2+</sup> ] <sub>i</sub> outflow and inhibits ERK1/2 pathway	Bone regeneration		[187]		



**Table 2** (continued)

Disease types	Polarized direction	Targets and strategies	Potentially polarized mechanism	Application	References
			FA-PEG-R-NPs@siERN1 deliver siERN1 to interfere with IP3R1/3 pathway to reduce $[Ca^{2+}]_i$	RA/IBD therapy	[188]
		Amino acid	Au@ZIF-8 enhances GS activity to elevate glutamine and alter other metabolic pathways	Metabolic diseases	[189]
			PEKK-L reemerges MET signaling to modulate Arg and energy metabolism	Bone regeneration	[190]
M1-related	M2-to-M1	RONS, Inducing RONS production	tTDCR NPs burst ROS	Cancer	[164]
			DMON-SNO mediates NO production	Cancer	[166]
		Iron, Delivering iron	SPF releases iron to induce oxidative stress	Cancer	[191]
			PEG-Fns release iron to induce ROS production	Cancer	[192]
			HION@Macs degrade into iron to activate the NF- $\kappa$ B pathway	Cancer	[193]
		Amino acid	DON blocks glutamine metabolism to upregulate M1 TAMs	Cancer	[194]
		Lactate, Metabolizing lactate	DL@NP-M-M2pep delivers DL to block PI3K/Akt and activate the NF- $\kappa$ B pathway	Cancer	[195]
			Lox-loaded Gd/CeO <sub>2</sub> @ZIF-8 depletes lactate	Cancer	[196]
			<i>E. hallii</i> -loaded E@Fe-DOX metabolizes lactate to butyrate	Cancer	[197]

pathways in resting cells [72, 73]. Transient  $Ca^{2+}$  influx facilitates OXPHOS and ATP production, whereas prolonged influx disturbs several dehydrogenases of the TCA cycle and ATP synthase and triggers increased opening of mitochondrial permeability transition pores (mPTPs), which damages OXPHOS to burst ROS and form a positive feedback loop between  $Ca^{2+}$  and ROS, where ROS enhances  $Ca^{2+}$  influx and vice versa, initiating glycolysis to activate the M1 phenotype [74, 75].

Consistent with their opposing immune responses, M1-polarized macrophages undergo a large-scale metabolic rewriting, accompanied by various metabolite changes compared with M2 macrophages [76, 77], which can be summarized in the following categories: (1) Interrupted TCA cycle, upregulated PPP, and other alterations damage OXPHOS, triggering ROS production; (2) The second metabolic breakpoint induces succinate accumulation and then burst of ROS via SDH-mediated succinate oxidation; (3) Enhanced IRG1 redirects citrate to itaconate, thus inhibiting SDH-mediated succinate oxidation to decrease ROS production; (4) Compensatory AASS and urea cycle are responsible for NO production; (5) Increased iNOS competes with Arg-1, metabolizing arginine into NO; (6) Glutamine anaplerosis forms  $\alpha$ -KG to fuel the first breakpoint at IDH1; (7) Persistent  $Ca^{2+}$  influx-induced  $[Ca^{2+}]_i$  overload impairs

mitochondrial function to produce mtROS; (8) Iron overload triggered by unbalanced iron transport leads to oxidative stress via iron-induced Fenton reaction; (9) IL-4 links anti-inflammatory function with upregulated FAO to support the M2 response; (10) IL-10 blocks the mTORC1 pathway and lowers the iNOS/Arg ratio to inhibit glycolysis; and (11) Lactate depletion orients toward the M2 phenotype despite contradictory conclusions.

Leveraging these metabolic parameters as underlying targets could guide the design of biomaterials for treating macrophage-driven diseases.

### 3 NM-Mediated Macrophage Activity Visualization and Fate Tailoring Based on Metabolic Parameters

According to the distinguishable metabolism in M1/M2 macrophages (Fig. 3), the subsequent sections in this article will systematically elaborate NM-traced macrophage behaviors relying on multiple imaging techniques and reorient the macrophage phenotype to tailor its fate for immunotherapy.

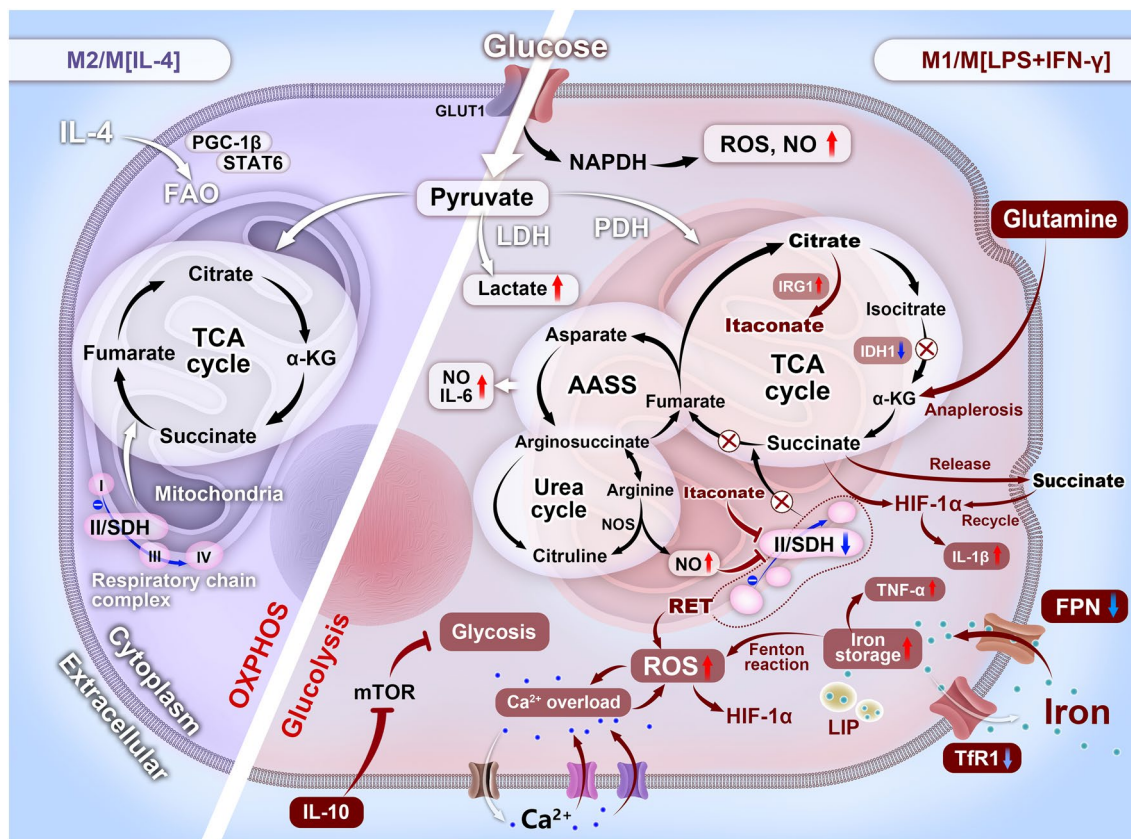


**Fig. 2** Metabolic adaptation in M1 and M2 macrophages in response to environmental cues: an underlying target for macrophage theranostics

### 3.1 RONS

#### 3.1.1 NMs Visualize RONS to Evaluate Macrophage Activity

ROS are considered a series of chemically active substances generated from intracellular oxygen through electron transfer, primarily including hydrogen peroxide (H<sub>2</sub>O<sub>2</sub>), hydroxyl radical (OH·), hypochlorous acid (HOCl), and superoxide anion (O<sub>2</sub><sup>·-</sup>) [78]. Under stimuli, resting macrophages are polarized to the M1 phenotype with glycolysis, a mode of increased ROS production [11], whereas the M2 phenotype favors OXPHOS to maintain the physiological activity of cells with less ROS production [79]. ROS act as a double-edged sword in modulating macrophage polarization [80, 81]. At low levels, ROS are beneficial for initiating macrophages with M2, whereas at high levels, ROS drive macrophage M1 polarization [82, 83].

With the help of interdisciplinary strategies, a well-designed fluorescent “off-on” framework is opening the door for real-time imaging of living cells [84–87]. The

traditional ROS imaging strategy involves applying fully- or semi-synthetic dyes, which emit fluorescence when oxidized by ROS [88]. H<sub>2</sub>O<sub>2</sub> is the most stable and abundant endogenous ROS and acts as the precursor for producing other ROS at concentration ≥ 1 mM [89, 90], such as HClO [91]. Mao et al. [92] designed a ratiometric two-photon quinolone skeleton-based probe via covalent cross-linking, containing oxathiolane as the HClO identification part, which rapidly responded to HClO by oxidizing oxathiolane in macrophages, accompanied by a shift in absorption peak from 492 to 563 nm, thus monitoring overgeneration of HClO in macrophages. This probe has unparalleled advantages, such as less light drift and background signal and higher spatiotemporal resolution than single fluorescence-based probes. Semi-synthetic dyes seem to be more attractive due to their simple synthesis from commercially available dyes, which are used for ROS imaging in macrophages, such as IR-780 iodide [93], 1,8-naphthalimide [94], and fluorescein [95].

Photoacoustic (PA) imaging with high spatial resolution and deep tissue penetration has been applied to track

macrophage activity [96, 97]. Xing et al. [98] embedded ROS-responsive hydrocyanine substrate (HCy5) and RNS-responsive cyanine substrate (Cy7) onto lanthanide-doped nanocrystal surface via hydrophobic interactions to construct core-shell upconversion nanoprobe (size ~ 100 nm). These combined with multispectral photoacoustic tomography could ratiometrically trace RONS in RAW 264.7 cells due to the structural rearrangement or degradation of HCy5/Cy7, accompanied with altered absorbance at 640 or 800 nm, respectively, thus revealing the pathophysiological process in LPS- or acetaminophen (APAP)-induced inflammatory mice (Fig. 4a). The strategy monitors endogenous ROS/RNS distribution and alterations, mapping out the pathological process to advance high-throughput drug screening. Limited by the poor penetrability and stability of probes in vivo [86, 99], MRI has received more attention in cell imaging due to its high spatial resolution, almost zero background signal, and unrestricted signal penetration depth [100]. Our group [84] synthesized Mn-doped mesoporous silica nanoparticles (NPs) (diameter 110 nm) by an in situ hydrothermal method, which rapidly released  $Mn^{2+}$  once exposed to ROS to enhanced MRI signal. Thus, ROS imaging could be performed in macrophages derived from acute liver failure and acute pancreatitis mice. The strategy indicates that macrophage-centered diseases can be monitored using MRI-mediated ROS imaging. Sensor technology has broad prospects in macrophage imaging due to its high sensitivity, simplicity, speed, and cost-effectiveness [101]. Kumar et al. developed WaveFlex-structure sensors to monitor various biomarkers [102–107], such as alanine aminotransferase [108], providing valuable reference for tracking metabolic parameters through well-designed sensors.

Macrophages defend themselves against NO damage by forming a storage or transport system, but this protective mechanism may fail in an inflammatory state [14]. LPS(+ IFN- $\gamma$ )-activated M1 macrophages are characterized by significantly elevated NO, which is 30-fold higher [20, 109] than that in M2 macrophages [8, 45, 61], where NO induces nitrate stress [110]. Recently, exploiting probes to timely image NO for tracking macrophage behavior has attracted great attention, such as the *o*-diaminobenzene unit [111–113], *N*-nitrosation of secondary amines [114–117], and reductive deamination [118, 119]. Nagano et al. did pioneering work in NO imaging probes by introducing *o*-diaminobenzene [111, 120]. The unit has flourished among several researchers.

Yuan et al. [121] first synthesized an NO-responsive NIR-II probe with an *o*-diamine unit (NRP) by multiple cross-coupling reactions and loaded it into amphiphilic block copolymer to self-assemble nanoprobe (NRP@MPHCQ) with a diameter of 34.8 nm. The secreted NO in LPS + IFN- $\gamma$ -induced RAW264.7 cells oxidized the NRP unit from a weak electron acceptor into a stronger acceptor along with increased absorbance at 600–1000 nm, enabling NRP@M-PhCQ to visualize the migration and polarization of M2 macrophages for tracking early 4T1 cell-bearing tumor metastasis (Fig. 4b). This approach specifically targets M2 macrophages and tracks their polarization with noninvasiveness and deep penetration and provides insights for detecting and inhibiting early tumor metastasis. To overcome the limitations of *o*-diamine units, *N*-nitrosifying secondary amines were introduced in the following research [122, 123]. NO further interacts with  $O_2^{\cdot-}$  to produce a more cytotoxic peroxynitrite ( $ONOO^-$ ), with an aberrant formation rate ( $6.7 \times 10^9 M^{-1} S^{-1}$ ) in the inflammatory microenvironment [78, 122, 124]. Researchers have developed a series of nanoprobe for imaging intracellular  $ONOO^-$  to unveil macrophage behaviors [125, 126].

To sum up, these imaging techniques have huge potential in noninvasively visualizing RONS in macrophages to reveal diseases progression. Cost-effective fluorescent technologies cannot avoid background interference, deviating from true results and hindering translation to the clinic. Clinic-utilized technologies, such as MRI, enable analysis of these metabolites with deep penetration and highly programmed accuracy to supply reliable pathologic information, but is limited by high-cost and time-consuming tests. The following questions are often posed in imaging analysis in vivo: (1) Do probes only accumulate in specific macrophage subtypes? (2) How to orthogonally image the dynamic changes of different RONS and tailor their relationship during pathophysiological processes in real time? (3) Is the current single imaging modality for a single target susceptible to environmental interference? Multimodal probes simultaneously complete at least two imaging processes, which might break through the limitations of single imaging mode in vivo and integrate the advantages of various imaging techniques to achieve satisfactory imaging effects [127–129], perhaps serving as a banner to guide future research. Theoretically, intelligent

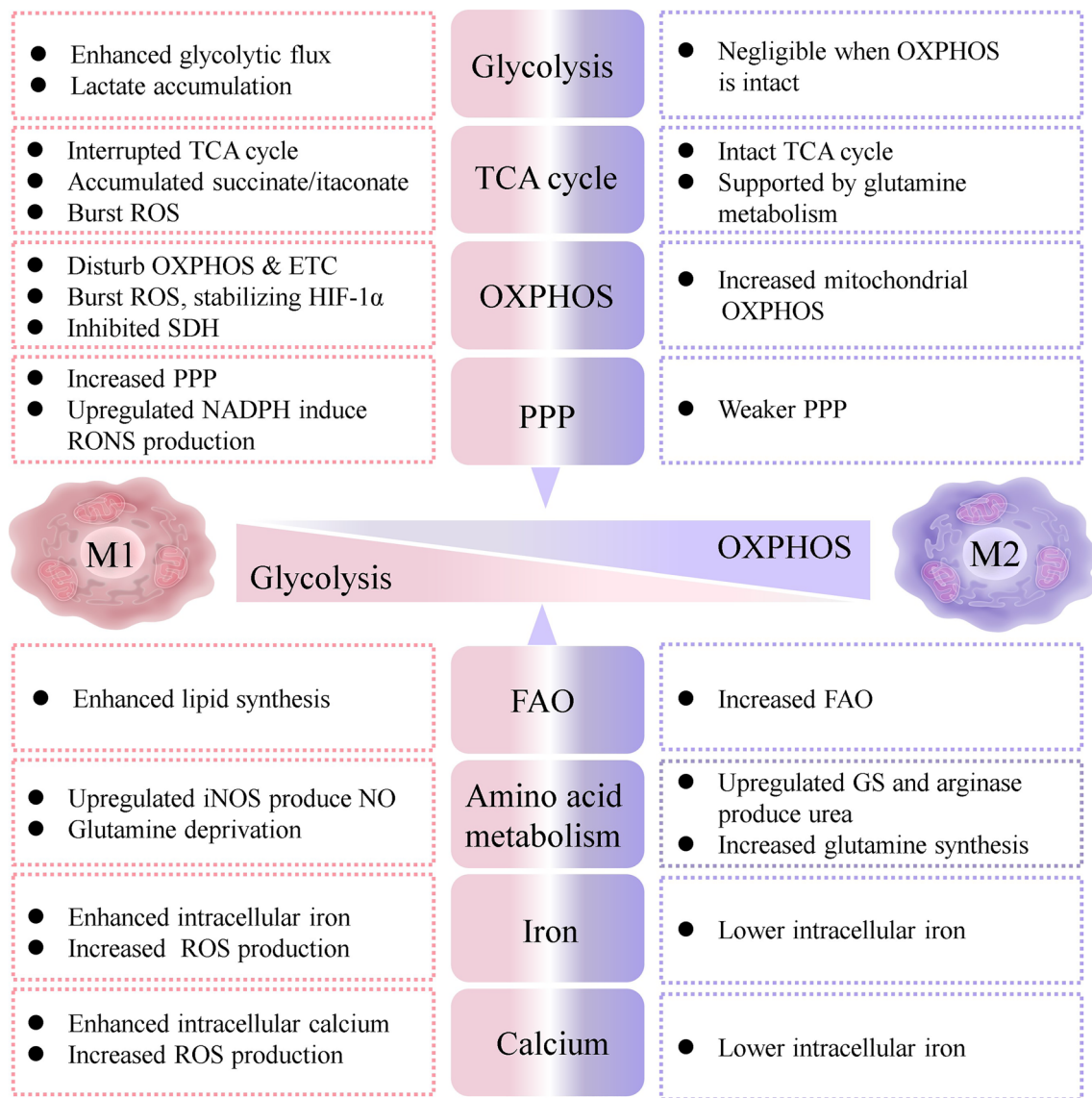


**Fig. 3** Schematic of distinguishable metabolic signatures of macrophage phenotypes

probes must identify differences between macrophages and other cells, as well as differences in diverse macrophage subtypes, to visualize macrophage behaviors [130].

### 3.1.2 NMs-Educated Macrophage Fate Based on RONS

M1 macrophage activation is closely associated with upregulated TNF- $\alpha$ -mediated inflammatory pathways [131–133], such as the downstream mitogen-activated

protein kinase (MAPK) and nuclear factor kappa-B (NF- $\kappa$ B) pathways [134]. Overall, RONS-scavenging down-regulates inflammatory cytokine levels to modulate M2 polarization mainly through the following mechanisms: (1) Significantly reducing the nuclear translocation of p65 NF- $\kappa$ B by inhibiting I $\kappa$ B phosphorylation, which inactivates the NF- $\kappa$ B pathway to silence inflammatory genes, including iNOS [135, 136]; (2) Attenuating the phosphorylation of AMPK (ERK, JNK/SAPK, p 38), thus blocking the MAPK cascade; and (3) Inhibiting STAT-1 phosphorylation to deactivate the JAK/STAT-1 pathway [132, 137–139]. Conversely, RONS supplementation can

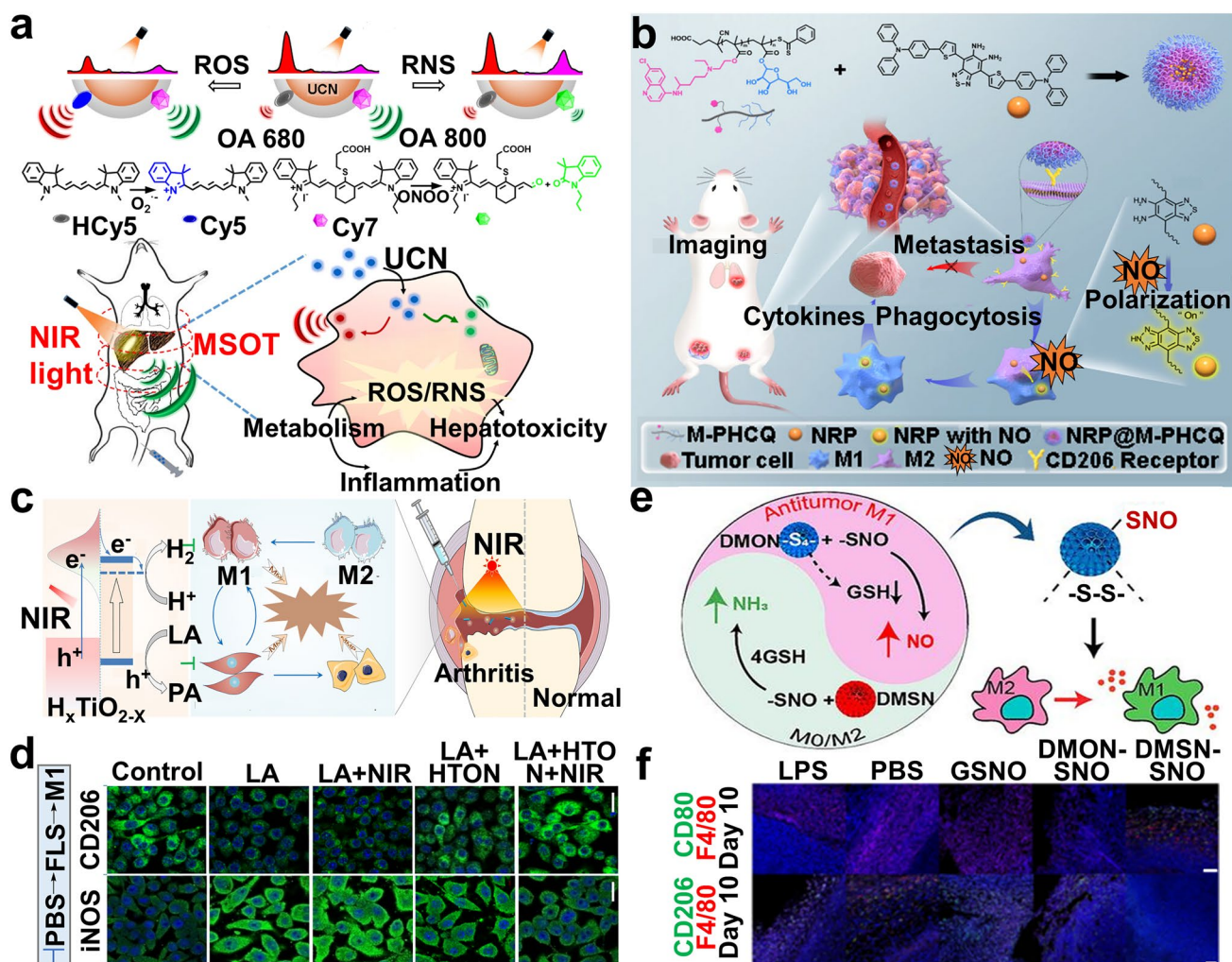


**Fig. 4** **a** NIR-responsive UCN visualizing endogenous RONS biomarkers in vivo [98]. Copyright 2019, Springer Nature. **b** Schematic of NRP@M-PHCQ fabrication, NIR-II imaging, and TAM repolarization based on secreted NO [121]. Copyright 2023, American Chemical Society. **c** NIR photocatalytic regulation of arthritic synovial microenvironment with HTON. **d** The effect of HTON photocatalysis on LA/FLS-stimulated macrophages [163]. Copyright 2022, American Association for the Advancement of Science. **e** DMON-SNO releases NO to modulate macrophage polarization. **f** IF staining of F4/80<sup>+</sup> CD80<sup>+</sup> and F4/80<sup>+</sup> CD206<sup>+</sup> cells in tumor tissues on day 10 after NPs injection [166]. Copyright 2022, American Chemical Society

stimulate these signaling pathway to deteriorate the M1 inflammatory response for tumor therapy [140].

Inspired by the dual role of RONS in macrophage activation, NM-mediated metabolic reprogramming, by regulating RONS levels to activate the required phenotype, has attracted increasing attention in disease therapy [141–146]. The methods that NM-manipulated RONS levels primarily focus on the following categories: (1) Natural antioxidants, such as glutathione peroxidase (GSH-Px) and superoxide dismutase (SOD) [147, 148]. Mao et al. [149] assembled SOD, catalase, and tannic acid (TA) into a spherical nanocomplex (TSC,  $\approx 50$  nm) via multiple noncovalent

interaction between TA and proteins. TSC effectively maintained enzymatic activity and was positively targeted to mitochondria, which scavenged mtROS in H<sub>2</sub>O<sub>2</sub>-activated L02 cells and liver tissues (detected by MitoSOX or DHE probes) through the antioxidant cascade, thus restoring mitochondrial function and blocking the inflammatory cascade to exert hepatoprotective efficacy of APAP-induced liver injury and LPS/D-gal-induced acute hepatic failure mice, as measured by Annexin V-FITC/PI, flow cytometry, western blotting (WB), and H&E staining. This strategy develops a TA-based mitochondrial targeted nanoplateform rather than membrane potential-dependent, opening new paradigms in

curing mitochondrial-related diseases. (2) Natural enzyme-mimicking synthetic NMs, such as  $\text{Cu}_{5,4}\text{O}$  [150, 151],  $\text{CeO}_2$  [152–155], and Pt [156–158]. Hu et al. [159] mixed  $\text{Ce}^{3+}$  with the  $\beta$ -cyclodextrin-engineered hyaluronic acid (HA) framework to form ultrasmall  $\text{CeO}_x$  (3–5 nm) via the nucleation site of carboxylic groups, finally constructing spherical  $\text{HA}@\text{RH-CeO}_x$  micelles with a diameter of 200 nm, which accurately targeted LPS-induced RAW264.7 cells and released Ce with SOD-like enzymatic activity to scavenge ROS, detected by flow cytometry and confocal laser scanning microscopy (CLSM), thus downregulating inflammatory signals to drive M2 repolarization for incomplete Freund's adjuvant (IFA)/collagen-induced RA mice therapy, measured by RT-qPCR, WB, CLSM, and immunofluorescence staining. The strategy resolves some challenges of  $\text{CeO}_x$ -based nanozymes in regulating redox homeostasis, such as rapid clearance, and cytotoxicity caused by organic solvent-mediated nanozymes dispersion. (3) Antioxidative substances, including vitamin E/C, gases (e.g.,  $\text{H}_2$ ,  $\text{H}_2\text{S}$ ), and polyphenols [147, 160, 161]. Hydrogen ( $\text{H}_2$ ) is considered an antioxidant because it selectively scavenges highly cytotoxic radicals (e.g.,  $\text{OH}\cdot$  and  $\text{ONOO}^-$ ) rather than the physiological ROS involved in cell signaling [162]. Zhao et al. [163] incorporated  $\text{H}_2$  into  $\text{TiO}_2$  nanorods to prepare monodisperse  $\text{H}_2$ -doped  $\text{TiO}_2$  ( $\text{H}_x\text{TiO}_{2-x}$ ) nanorods (HTON) by a full-solution method, achieving NIR-catalyzed  $\text{H}_2$  production due to a narrower bandgap of 1.45 eV, which scavenged ROS in LPS-induced RAW 264.7 cells and facilitated M2 repolarization, as detected by RT-qPCR, IF, and fluorescent staining, thus promoting photocatalytic synovial microenvironment regulation for complete Freund's adjuvant (CFA)/collagen-induced arthritis (CIA) therapy in mice (Fig. 4c, d). The inexhaustible HTON enabled efficient NIR-photocatalysis on demand and continuously released  $\text{H}_2$  for long-term and reproducible therapy while avoiding toxic side effects. Conversely, excessive RONS reprogrammed TAMs from the M2 to M1 phenotype to ameliorate the immune tumor microenvironment (iTME) against tumor [140, 164, 165]. Yu et al. [166] modified tetrasulfide-bridged organosilica NPs with thiol and then generated *S*-nitrosothiol (SNO) by  $\text{NaNO}_2$ -mediated thiol nitrosation, to synthesize porously dendritic nanostructured organosilica NO donors (DMON-SNO) with a size of  $\sim 230$  nm, which increased NO delivery in IL-4-induced bone marrow-derived macrophages (BMDMs)/RAW264.7 cells, detected by Griess reagent and DAF-FM probe. The released NO could interfere with

mitochondrial function in macrophages, thus activating M1 macrophages to hinder tumor growth in 4T1 cell-bearing mice. The macrophage phenotype was detected and quantified by flow cytometry, ELISA, WB, and RT-qPCR (Fig. 4e, f).

Each antioxidant method has its advantages and disadvantages, and its specific scenario should be considered when using it. Naturally occurring antioxidant enzymes are susceptible to the disease microenvironment, leading to inferior RONS-scavenging efficiency [167]. Antioxidative substances exhibit low ROS scavenging efficiency and poor bioavailability due to rapid metabolism and dissipative oxidation resistance [168]. Strategies for regulating RONS are mostly focused on synthetic metal-containing nanozymes with excellent antioxidative properties, which may potentially cause cytotoxicity due to undegradable metal elements and thus require further investigation. Green RONS-scavenging or supply platforms should be exploited to satisfy low toxicity, high biocompatibility, and sustainability issues. For example, the unique photosynthetic properties and easily functionalized surface of microalgae enable them to become an ideal candidate to construct a green RONS-scavenging platform [169] for disease therapy, such as diabetic wounds [170].

### 3.2 Succinate Metabolism

In 2013, a comprehensive metabolic map profiling derived from Tannahill et al. revealed that sharp succinate accumulation in LPS-stimulated BMDMs directly damaged PHD activity to stabilize HIF-1 $\alpha$ , which drives the expression of IL-1 $\beta$  and other HIF-1 $\alpha$ -dependent genes, acting as an endogenous inflammatory signal to elucidate innate immunity [198, 199]. SDH, also termed complex II, is a hub that links OXPHOS to electron transport. Intriguingly, LPS-induced mitochondrial hyperpolarization and enhanced SDH-mediated succinate oxidation collectively repurpose mitochondrial metabolism, leading to ROS burst via reversed electron transfer (RET) by forcing electrons back into complex I. This process upregulates the proinflammatory gene profile to drive the M1 response [11, 200]. This phenomenon is reversed by potent SDH inhibitors, malonate derivatives, dimethyl malonate (DMM), which can rapidly hydrolyze to malonate intracellularly, blocking succinate-dependent ROS production and recovering

pro- or anti-inflammatory gene homeostasis (IL-1 $\beta$ , IL-10, and IL-1RA) to remodel mitochondrial metabolism. This could be a valuable strategy to achieve M1 to M2 polarization. Valls-Lacalle et al. [176] revealed that pretreating reperfusion-injured mice with DMM in a concentration-dependent manner (0.03–30 mmol L<sup>-1</sup>) decreased the infarct size (24.57  $\pm$  2.32% vs. 39.84  $\pm$  2.78%) by blocking SDH-mediated ROS production and mPTPs. As an attractive target for regulating macrophage metabolism, unlike RONS, which have been extensively studied, researchers need to explore NM-modulated succinate oxidation to address this gap in our understanding of defense against diseases.

### 3.3 Itaconate Metabolism

#### 3.3.1 NMs Visualize Itaconate to Evaluate Macrophage Activity

Macrophages maintain a physiological pool of itaconate against inflammatory damage. The itaconate level in resting macrophages is as low as the micromolar level compared with > 1 mM in LPS-stimulated macrophages, possibly due to the elevated IRG1-mediated itaconate synthesis [201, 202]. In 2019, Wang et al. [203] introduced the Ac<sub>4</sub>ManNAz moiety to develop a thiol-reactive probe, 1-OH-Az, which systematically quantified and profiled itaconate-targeted cysteine sites in proteomes of RAW 264.7 cell lysates, in combination with quantitative chemoproteomic technology. They identified 260 itaconate-modified cysteines and found that itaconate inhibits glycolysis primarily by silencing glycolytic enzymes (e.g., ALDOA) to alleviate the inflammatory response in activated macrophages and revealed the negative feedback between glycolysis and the anti-inflammatory mechanism originating from itaconate. Nonetheless, this profiling method only indirectly monitors itaconate-modified cysteines in cell lysates [203]. Itaconate-alkyne bio-orthogonal probe (ITalk) was developed to directly enter cells [204] and achieve quantitative and site-specific chemoproteomic profiling of itaconate. They identified 1926 targets of itaconate involved in inflammation-related pathways and provided abundant data for understanding the role of itaconate in macrophages. However, the study was limited by itaconate-monitoring techniques (GC-MS) that failed to monitor the concentration distribution of itaconate in different intracellular regions. An innovative study designed a

genetically encoded fluorescent biosensor (BioITA) to timely detect the itaconate dynamics curve at subcellular resolution in macrophages isolated from LPS-bearing mice [205]. The altered fluorescence intensity revealed itaconate fluctuations under inflammatory conditions, making it a powerful tool for imaging itaconate with temporal-spatial resolution in living macrophages.

Given that its anti-inflammatory efficiency, it is of great significance to develop biological probes to achieve itaconate-monitoring in macrophages to deepen our understanding of the unknown biological functions about itaconate. The current monitoring methods inevitably are dependent on liquid chromatograph mass spectrometer (LC-MS) and rarely directly obtain itaconate dynamic in macrophages, and more in-depth studies are needed to fill this relatively blank field.

#### 3.3.2 NM-Educated Macrophage Fate Based on Itaconate

Itaconate (IA) is highly generated in stimuli-induced macrophages and mediates the cross-talk between immunity and metabolism as an anti-inflammatory metabolite to negatively regulate the inflammatory response and govern M2 polarization in vitro and in vivo via multiple mechanisms [206–208]: (1) It inhibits SDH activity by blocking RET-dependent ROS production at complex I, thereby inhibiting HIF-1 $\alpha$  activity and IL-1 $\beta$  production, and subsequent, inactivating the NLRP3 inflammasome [11, 207]. (2) It alkylates residues of KEAP1 via Michael addition to upregulate the expression of Nrf-2, due to the presence of electrophilic  $\alpha$ ,  $\beta$ -unsaturated carboxylic acid [209]. (3) It induces electrophilic stress to inhibit I $\kappa$ B $\zeta$  translation that regulates secondary transcription via upregulated ATF3 but not Nrf-2, described as the I $\kappa$ B $\zeta$ -ATF3 inflammatory axis [210]. (4) It dephosphorylates IL-23, failing to bind to the IL-17 gene promoter to inhibit downstream IL-17 transcription [178]. (5) It inhibits the NF- $\kappa$ B pathway [211].

The properties of itaconate provide a novel direction for exploiting immunometabolism-based disease intervention strategies. Mechanically, the strategy that rewrites itaconate metabolism for achieving additional benefits is primarily dependent on delivering itaconate into macrophages in a locally on-demand manner. Yu et al. [212] fabricated monodisperse hydrogel microspheres by the self-assembly of zinc ions, 2-methylimidazole, and IA (IA-ZIF-8@HMs) (diameter

20.25 ± 0.43 μm) via one-step microfluidic technology under ultraviolet light. These sustainably released itaconate under the acidic environment of lysosomes and exerted excellent anti-inflammatory and antioxidative stress damage *in vitro* and *in vivo* for mono-iodoacetic acid-induced OA mice therapy (analyzed by ELISA, H&E staining, and O-fast green staining). Nevertheless, limited by the poor cell permeability of itaconate, it is necessary to develop functionally similar itaconate derivatives (dimethyl itaconate [DMI] [177] and 4-octyl itaconate [4OI] [213]) or itaconate-loaded NMs. Nakkala et al. [178] synthesized DMI-encapsulated poly-ε-caprolactone nanofibers by electrospinning technology to downregulate the IL-23/IL-17 inflammatory axis-related genes via the IκBξ-ATF3 axis and upregulate the antioxidant Nrf-2 target genes in LPS/IFN-γ-stimulated RAW 264.7 cells and BMDMs, thereby rewriting itaconate metabolism to polarize the M1-to-M2 phenotype and relieve inflammation against MI (Fig. 5a, b). The percentage of M1/M2 macrophage *in vitro* or *in vivo* were assessed by ELISA, flow cytometry, IF, and PCR. The study unveils the potential metabolic regulatory function of DMI on macrophages in the tissue microenvironment.

However, these derivatives may be insufficient to mimic endogenous itaconate. No conclusive evidence confirms that their therapeutic action is derived from itaconate, and no real consensus exists about how to effectively deliver itaconate intracellularly [206]. The burgeoning field of delivering itaconate via biomimetic carriers to alter intracellular itaconate metabolism may be confronted with great development potential and challenges. Moreover, the role of itaconate in M1 macrophages has been unambiguously investigated, whereas the role of itaconate as an M2 macrophage inhibitor has been scarcely studied [214–216].

### 3.4 Iron Metabolism

#### 3.4.1 NMs Visualize Iron to Evaluate Macrophage Activity

Iron is an essential trace element that participates in multiple metabolic processes [217, 218]. Macrophages play a core regulatory role in iron homeostasis according to their unique genetic program [219]. Opposite iron metabolism operates in macrophages: iron is sequestered in M1 macrophages against bacterial infection [220], whereas it is released in M2 phenotype to facilitate tissue repair but may promote

tumor growth [70, 221]. Tracking iron metabolism to evaluate macrophage activity to understand disease progression is a promising prospect and remains challenging.

Benefiting from noninvasiveness, spatiotemporal optical readout, and low-cost, fluorescent technologies have emerged to track iron homeostasis, such as LIP, which triggers Fenton reaction-induced oxidative stress and oppositely expresses in M1/M2 macrophages [222]. Xing et al. [223] designed a fluorescent probe by covalently coupling coumarin 343 (fluorophore) and 3-nitrophenylazanyl ester to visualize the activation of M1 and M2a macrophages by monitoring LIP levels via a photoinduced photon transfer mechanism induced by Fe(II)-activated N–O bond cleavage. This technology provides insights for imaging iron using fluorescent technologies under pathophysiological conditions. Macrophages containing abundant hemosiderin exhibit high MRI contrast. Limited by susceptibility to interference from background signals of fluorescence, MRI was utilized to investigate iron behaviors in macrophages [224, 225]. However, the slow imaging speed and high-cost limit its application. Secondary ion mass spectrometry (SIMS) was used to for iron analysis, even at low concentrations [226–228]. Lovric et al. developed SIMS imaging to explore the uptake and subcellular localization of iron in alveolar macrophages, providing discernment and therapeutic strategies on iron metabolism at the subcellular level to reduce the cytotoxicity of iron overload [228]. Although SIMS can track iron with high sensitivity and spatial resolution (up to 37 nm), it is a new technology and rarely used due to the need for expensive instrumentations and time-consuming testing, similar to MIR. Moreover, macrophage behaviors are dynamic, whereas current monitoring methods can only be fixed at a certain time and environment. How to dynamically monitor metabolites has not been fully investigated, which motivates researchers to develop methods for dynamically tracking them in biological systems.

#### 3.4.2 NM-Educated Macrophage Fate Based on Iron

Iron overload activates M1 macrophages to fine-tune the innate immune response and iron deprivation may block M1 [71]. Generally, iron levels manipulate REDOX homeostasis intracellularly. Capturing excessive iron can inhibit ROS formation to drive M2 polarization by silencing inflammatory pathways (e.g., NF-κB) [229], whereas

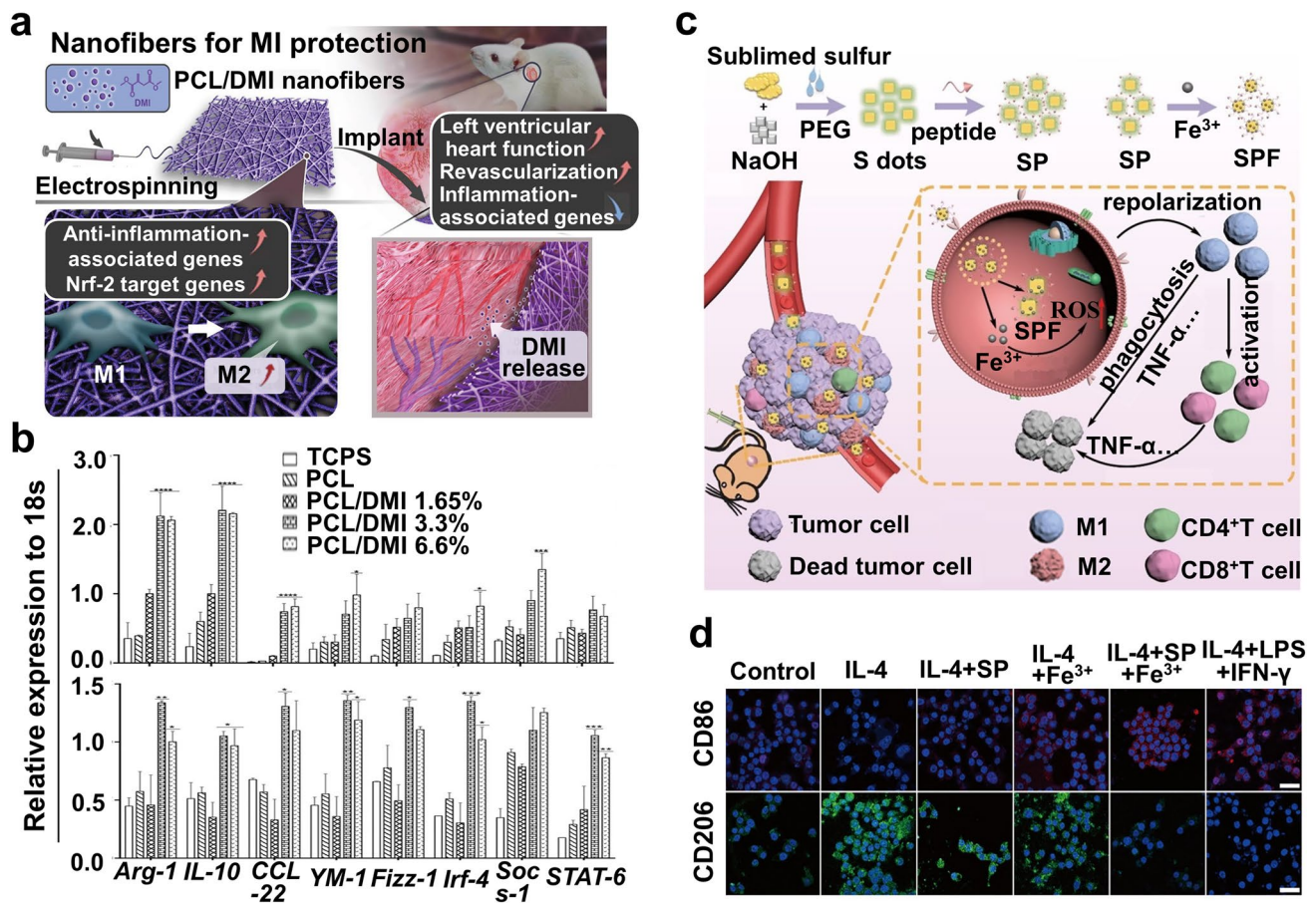


**Fig. 5** **a** Schematic illustration of DMI-loaded PCL nanofibers and modulating M1-to-M2 macrophage polarization. **b** The M2-related gene expression of RAW 264.7 cells (upper) and BMDMs (lower) after treatment with different groups for 24 h [178]. Copyright 2021, Wiley-VCH GmbH. **c** Schematic of SP/SPF formation and SPF reeducates TAMs from M2 to M1 for cancer immunotherapy. **d** IF staining of CD86 to M1 and CD206 to M2 in LPS-induced RAW 264.7 cells after different treatments [191]. Copyright 2021, American Chemical Society

iron replenishment induces oxidative stress to activate pathways, such as NF- $\kappa$ B, upregulating the inflammatory cascade to initiate the M1 response [221, 230, 231].

Researchers have extensively investigated on shaping the macrophage phenotype by reprogramming iron metabolism, including iron-scavenging and supply, for curing macrophage-driven diseases [232]. Zhu et al. [179] designed dual-functional macromolecular poly(catechol) nanoscavengers loaded with deferoxamine via the self-assembly with a particle size of  $36.2 \pm 7.6$  nm, simultaneously chelating excess iron and relieving iron-induced oxidative stress in RAW 264.7 cells, thus protecting mice with intracerebral hemorrhage (ICH). Iron levels were adopted via CLSM and flow cytometry (Perl's staining). This delivery carrier addresses the dose-limiting toxicity using

chelators alone and achieves long-term stable release, providing a clue for iron-depleting therapeutic regimen. Similarly, iron dextran therapy resolved kidney macrophage iron depletion by supplying LIP and downregulating TfR1, which polarizes macrophages toward M1 for chronic kidney disease therapy [233]. Much of the observed therapeutic effects of regulating iron metabolism can be traced to tumor therapy. Contrary to iron-scavenging driving the M2 phenotype against inflammation, repolarizing TAMs from M2 to M1 by replenishing iron is believed to be an attractive strategy against tumors [234, 235]. Sang et al. [191] modified S dots (synthesized by an  $O_2$ -assisted top-down method) with TAM-targeted peptides to construct ultrasmall nanotraps (SP) with a size of 3.2 nm, which positively adsorbed and internalized endogenous iron into TAMs,

attributed to the plentiful iron-binding sites on SP surface by coordinating with oxygen. SP-derived iron produced ·OH and NO in IL-4-induced BMDMs/RAW264.7 cells, detected by CLSM (·OH, DCFH-DA probe) and Griess kit (NO), which remodeled M2-to-M1 phenotype and formed a positive feedback loop between ROS production and M1 polarization, thus delaying 4T1-bearing breast tumor growth (Fig. 5c, d). The M2-to-M1-polarized behavior was detected through protein and gene levels by IF, flow cytometry, ELISA, WB, and immunohistochemical staining (HC). The nanotrap effectively targeted into TAMs and avoided excessive exogenous iron-caused cytotoxicity, providing opportunities to utilize endogenous substances against various diseases. Similarly, iron oxide NPs can be degraded to iron ions in the lysosomes of macrophages and induce oxidative stress to trigger the M1 response [193, 236, 237].

Iron regulator-loaded nanocarriers release regulators to manipulate oxidative stress intracellularly for disease therapy. However, uncontrollable release in other macrophage phenotypes or cells causes dose-dependent toxicity, which attributes to nonspecifically chelate physiologically essential iron. Modifying these nanocarriers with stimuli-responsive moieties may be a charming avenue to achieve targetable cellular internalization, drawn-out circulation half-time, long-term regional enrichment, and sustainable release [238]. It may be more in line with the on-demand release requirements in specific sites compared with direct physical release [192].

There are contradictory reports concerning its precise effects. Dietary iron overload in mice induces hepatic and peritoneal macrophage M2 polarization and inhibits the M1 phenotype [239]. Iron-incubated macrophages induce the translocation of NF- $\kappa$ B p65 nuclear and inflammatory cytokine expression, which is consistent with other studies [240, 241]. These contradictory findings illustrate the complexity of the impact of iron metabolism on macrophage polarization.

### 3.5 Calcium Metabolism

Calcium is a crucial messenger that controls several cellular functions [242]. Prolonged  $\text{Ca}^{2+}$  influx impairs OXPHOS and phosphorylates certain enzymes (e.g., NOS), thereby facilitating the M1 response by stimulating NF- $\kappa$ B and MAPK pathways. Conversely, lowering intracellular calcium ( $[\text{Ca}^{2+}]_i$ ) levels reduces mtROS production and inhibits ERK

phosphorylation (MAPK-related), consequently downregulating proinflammatory factors and promoting M2 polarization [243–245]. Macrophage phenotypes link to  $[\text{Ca}^{2+}]_i$  levels, with elevated  $[\text{Ca}^{2+}]_i$  levels responding to M1 stimuli and reduced  $[\text{Ca}^{2+}]_i$  levels responding to M2 stimuli. Increasing attention has been focused on developing NM-regulated  $[\text{Ca}^{2+}]_i$  levels to remodel M1-to-M2 phenotype development for macrophage-driven immunotherapy [243, 246–249].

One strategy is to encapsulate  $\text{Ca}^{2+}$  regulators, such as EGTA [186] and BAPTA-AM [75], glutting excess  $[\text{Ca}^{2+}]_i$ , restoring ROS-mediated disordered mitochondrial homeostasis to inhibit M1 activation against  $\text{Ca}^{2+}$  overload-driven diseases. Kang et al. [185] loaded  $\text{Ca}^{2+}$  regulators (supplier DMNP-EDTA- $\text{Ca}^{2+}$  or chelator BAPTA-AM) into mesoporous silica-decorated upconversion NPs to prepare UCNP@mSiO<sub>2</sub> with a diameter of  $58 \pm 6$  nm. This was further modified with the Arg-Gly-Asp (RGD) peptide-containing cap and photocleavable linker via cyclodextrin-adamantine host-guest complexation, which temporally enhanced or depleted  $[\text{Ca}^{2+}]_i$  (measured by Fura-2 AM probe) under NIR light by on-demand releasing  $\text{Ca}^{2+}$  regulators, remotely modulating RAW 264.7 cells with the M1 or M2 response to exert immune functions, as detected by IF, qRT-PCR. This system achieves intracellularly targetable uptake and time-dependent release. However, the underlying mechanism by which UCNP@mSiO<sub>2</sub>-resurged the M2 is unclear.

The other strategy is to block improper  $\text{Ca}^{2+}$  flow by interfering with related channels or signaling pathways [187]. Feng et al. [188] constructed a macrophage-targetable delivery system using polyethylenimine (PEI) and poly( $\beta$ -amino amine) (PBAA) as siERN1 carriers (FA-PEG-R (Peptide: RKKRRQRRR) - NPs (ss-PBAA-PEI)@siERN1) with a diameter of  $\sim 110.0$  nm through self-assembly, which released endoplasmic reticulum nucleus signaling 1 gene (siERN1) under pH 5.5/GSH to modulate  $[\text{Ca}^{2+}]_i$  levels (detected by flow cytometry and CLSM with fluo-4AM labeling) in LPS-stimulated RAW 264.7 cells by disturbing inositol 1,4,5-trisphosphate receptor 1/3 (IP3R1/3), thereby initiating M1-to-M2 polarization as demonstrated by WB, RT-qPCR to maintain immune homeostasis, demonstrating superior therapeutic efficacy in CIA and dextran sulfate sodium salt-induced IBD (Fig. 6a–c). This study confirms ERN1 as an effective target, providing promising insights into  $\text{Ca}^{2+}$ -regulated siERN1 drugs design and its potential mechanisms.

Cross-talk between macrophage polarization and  $\text{Ca}^{2+}$  occurs in multiple diseases. Manipulating  $\text{Ca}^{2+}$  signaling can be regarded as an underlying adjuvant therapy. Akin to iron,  $\text{Ca}^{2+}$  regulator-loaded nanovehicles modulate intracellular oxidative stress by altering  $[\text{Ca}^{2+}]_i$  to fine-tune macrophage fate. The uncontrolled release within non-specific cells inevitably leads to dose-determined toxicity, as it does interference with ion channels or signaling pathways. Moreover, the accurate mechanisms underlying its functionality remain poorly understood. Strengthening mechanistic understanding of  $\text{Ca}^{2+}$  signaling provides more opportunities to develop  $\text{Ca}^{2+}$ -based therapeutic approaches. Establishing an intelligent delivery system in terms of specific macrophage subpopulations by modifying targeted or stimuli-responsive moieties, achieving its oriented phagocytic uptake, prolonged regional enrichment, and spatiotemporal release as well as minimizing toxicity to adjacent cells remains a challenge.

### 3.6 Interleukin-4/10

#### 3.6.1 IL-4

The STAT pathway is associated with macrophage polarization [250, 251]. The IL-4-dependent STAT6 pathway responds to the M2 phenotype [9, 252–254]. In detail, IL-4 binds with its receptor to activate JAK2 downstream, inducing STAT6 phosphorylation and entering the nucleus to bind to promoter elements of IL-4-responsive gene, thus transcribing M2 lineage genes (e.g., *Il10*, *Arg-1*) to drive M2 differentiation, which acts as a vital immunoregulator to block inflammatory process [255–257]. Recently, IL-4 links anti-inflammatory potential to mitochondrial oxidative metabolism which was confirmed by Chawla et al. [77], who showed that IL-4-treated macrophages (known as M(IL-4)) strongly activated PGC-1 $\beta$  expression and upregulated FAO gene profiling (e.g., LPL) to promote M2 polarization, relieving macrophage-driven inflammation. Moreover, IL-4 and CSF-1 cooperatively enhance fatty acid synthesis (FAS)/FAO via the mTORC-IRF4 axis to support M2 polarization [258, 259]. Thus, M(IL-4) is closely associated with upregulated FAO.

Recognition of the anti-inflammatory potential of IL-4 paves the way for IL-4 supply from reasonable delivery platforms to drive macrophage polarization in some tissue engineering applications. Due to its short half-life of only several

minutes and dose-dependent toxicity [260], multiple loading platforms through physical adsorption or encapsulation and chemical coupling have been developed to deliver exogenous IL-4 to cells or tissue for clinical application [182, 261]. Our group [262] developed a multilayered defensive platform (IL-4@PEGRA NAs) with a size of  $96.45 \pm 7.3$  nm via the self-assembly of polycatechol-containing poly(ethylene glycol)-ylated phenolic rosmarinic acid (PEGRA) and IL-4, to preserve bioactivity and prolong circulation time. The platform delivered IL-4 into inflammatory tissues, achieving M1-to-M2 polarization in LPS-stimulated BMDMs and mice colon tissue in dextran sulfate sodium salt-induced acute colitis, thus protecting against IBD. The percentage of M1/M2 was measured by IF, flow cytometry, WB, and ELISA (Fig. 6d, e). The nanoarmor defended IL-4 against rapid biodegradation, prolonging circulation half-life, achieving triggered release, and avoiding immunogenic side effects. In addition to the aforementioned physical methods, Spieler et al. [263] genetically engineered an amino acid-incorporated IL-4 variant via genetic code expansion and then directly performed bio-orthogonal PEGylation (PEG-folate, a targeting moiety) by strain-promoted alkyne-azide cycloaddition to overcome the pharmacokinetic challenges of IL-4, which prolonged the half-life to 4 h in healthy mice and polarized primary murine macrophages toward M2 via RT-qPCR detection and accumulated into arthritic joints to cure antigen-induced arthritis mice.

#### 3.6.2 IL-10

IL-10 initiates an anti-inflammatory response mainly dependent on the JAK–STAT3 pathway [264–266]. Briefly, IL-10 binds with IL-10 receptor to activate JAK1, which stimulates STAT3 to translocate into the nucleus, thus combining with specific DNA sequence to initiate DNA transcription and upregulate M2-associated genes (TGF- $\beta$ 1, Mrc1) for anti-inflammatory cascades. Recently, IL-10 was verified to remodel glycolysis and potentiate OXPHOS by blocking glucose uptake and glycolytic gene expression. IL-10 reprogrammed metabolic processes by inhibiting mTOR complex 1 (mTORC1) signaling via STAT3 signaling and accelerated mitophagy to eliminate impaired mitochondria, thereby controlling inflammation [17, 26, 267, 268]. IL-10 blocked NO production in activated macrophages by silencing iNOS [269, 270] and upregulating arginase [271].

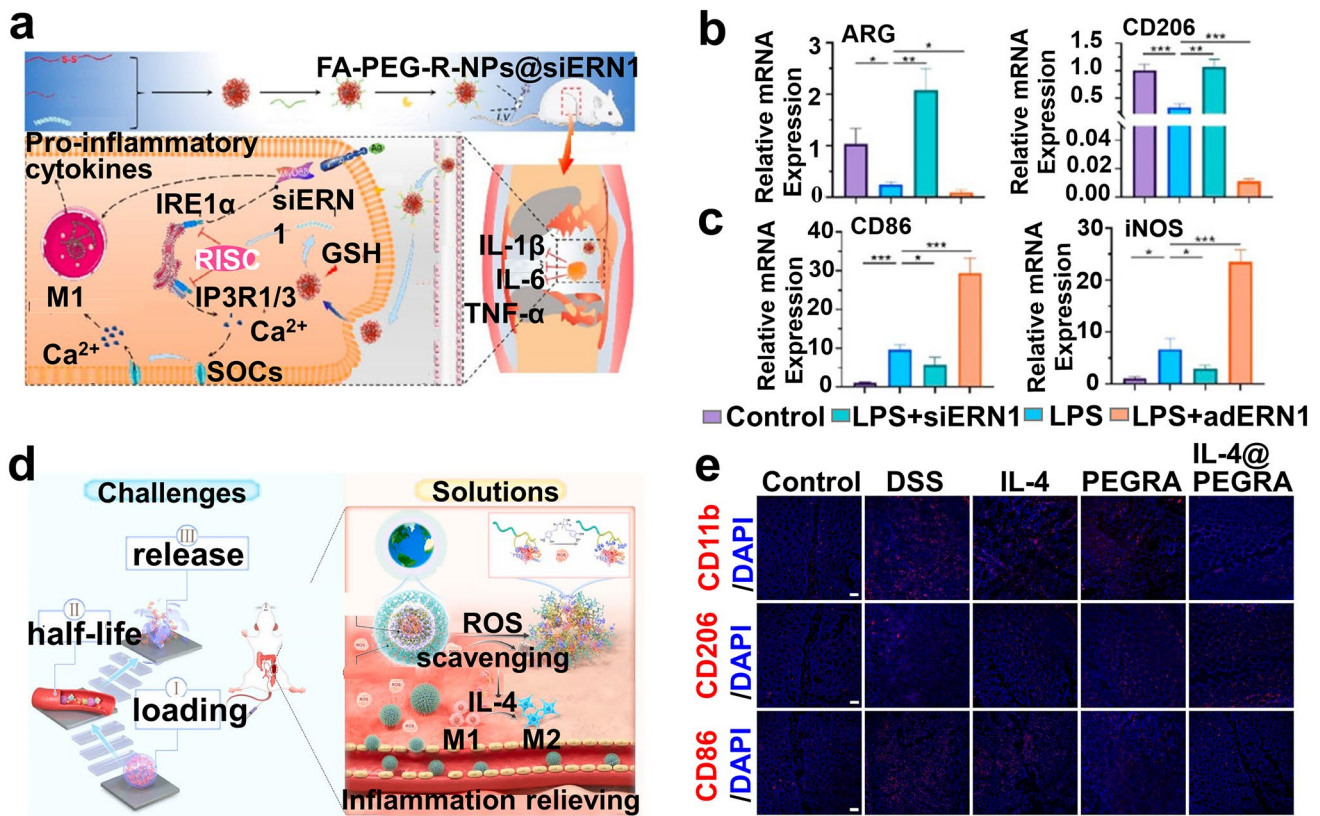


**Fig. 6** **a** Schematic diagram of delivered siERN1 promoting macrophage M2 polarization by interfering with IP3R and modulating [Ca<sup>2+</sup>]<sub>i</sub>. **b** M2 and **c** M1 marker expression levels detected via RT-qPCR [188]. Copyright 2021, American Chemical Society. **d** Schematic diagram of IL-4@PEGRA nanoarmor modulating M1-to-M2 polarization for IBD therapy. **e** IF staining of CD86<sup>+</sup>, CD206<sup>+</sup>, and CD11b<sup>+</sup> cells in colon tissue derived from IBD-bearing mice on day 10 after treatment [262]. Copyright 2023, Elsevier

Exogenous IL-10 supply blocks macrophage inflammatory cascade reaction to drive M2 polarization, exhibiting enormous bioregenerative potential [272, 6]. In line with IL-4, researchers are attempting to develop an IL-10-loaded nanoplatform, which releases IL-10 via physical or chemical stimuli-triggered mechanisms, paving the way for targeted delivery [183]. Extracellular vesicles (EVs) have attracted increasing attention as feasible drug delivery systems [273]. Tang et al. [184] designed an IL-10-packaged nanoplatform (IL-10<sup>+</sup> EVs) with a diameter of 134 nm by engineering dexamethasone-stimulated plasmid transfected-RAW 264.7 cells to avoid IL-10 degradation and target to the kidney. IL-10<sup>+</sup> EVs favored the M2 phenotype of LPS-induced BMDMs by inactivating mTOR1, followed by its downstream targets (e.g., S6K, S6), as detected by flow cytometry, RT-qPCR, and HC, and promoted mitophagy to maintain mitochondrial homeostasis against ischemic acute kidney injury

(AKI) (Fig. 7a, b). The versatile delivery strategy enabled IL-10 to evade phagocytosis, prolong circulation time, and decrease immunogenicity.

Overall, IL-4/10 link macrophages metabolism to their anti-inflammatory functionality. The major barriers, such as susceptibility to degradation and short circulation half-life, prevent IL-4/10 from being directly employed for diseases therapy. Physical encapsulation can effectively maintain the biological activity of IL-4/10, but hardly avoids their uncontrolled release. Conversely, chemical stimuli-triggered release may better satisfy the on-demand release needs while reducing off-target effect-induced side effects [274]. Current strategies have resolved pharmacokinetic challenges to some extent. However, bridging them with natural materials to exploit delivery platforms with high load efficiency, which can maintain their effective biological activity, as well as accurately orient exogenous IL-4/10 in targetable sites to

achieve long-term continuous release, remains a major challenge that requires more extensive exploration.

### 3.7 Amino Acid Metabolism

Metabolic adaptation in macrophages facilitates specific immunophenotype transformation [14, 275]. Among them, alterations in the metabolism of some amino acids are the earliest and foremost metabolic features that occur during macrophage polarization and define macrophage subtypes [276].

#### 3.7.1 Arginine

Arginine metabolism remodels macrophage phenotype via the iNOS/Arg-1 axis. M(IL-4)-derived mice upregulate Arg-1 activity, whereas similar results were not observed in human macrophages. Transcription factor Fra-1 reemerges M1 macrophages by silencing Arg-1 to enhance inflammation [277]. Arg-2, another enzyme involved in L-arginine metabolism, modulates mitochondrial dynamics to upregulate OXPHOS, polarizing M1 macrophages to M2 phenotype [278, 279]. Jiang et al. [190] engineered a liver-inspired polyetherketoneketone (PEKK) scaffold with a thickness of 30  $\mu\text{m}$  by femtosecond laser etching technology and sulfonation reaction. They reemerged hepatocyte growth factor receptor (MET) signaling in LPS-induced CVX-BMDMs/RAW 264.7 cells, followed by activating downstream Ras pathway, which promoted the retrograde transfer of Arg-2 from mitochondria into the cytoplasm and remodeled energy/arginine metabolism by enhancing OXPHOS to mobilize M2 phenotype for improving rat osteoporotic bone defect (demonstrated by flow cytometry, IF, ELISA, and RT-qPCR) (Fig. 7c–f). The strategic application of Arg-2 in this study verified its potential as an anti-inflammatory reserve to resurge M2 macrophages. The effect of PEKK on the isoenzyme Arg-1 has not been thoroughly studied, and it may inevitably lead to off-target effects on Arg-1. Nevertheless, there are contradictory viewpoint that Arg-2 stimulates the M1 response through mtROS and is responsible for inflammatory diseases.

#### 3.7.2 Other Amino Acids

The regulatory role and metabolic fate of citrulline remain unclear, although citrulline can be metabolized into argininosuccinate (an inflammatory mediator) by the citrulline–NO cycle. Citrulline rapidly declines in LPS(+ IFN- $\gamma$ )-primed BMDMs, and ASS1-mediated citrulline depletion is responsible for JAK2–STAT-1 signaling activation and proinflammatory cytokine generation, stimulating the M1 phenotype [280].

Carbon tracing indicates that one-third of the carbon in the TCA cycle metabolites of M2 macrophages derives from glutamine, which fuels the immune system [281], and serves as an anti-inflammatory metabolite to maintain M2 differentiation through the uridine diphosphate *N*-acetylglucosamine (UDP–GlcNAc) pathway and glutaminolysis-derived  $\alpha$ -KG [16, 281, 282]. Glutaminolysis-derived  $\alpha$ -KG activates M2 macrophages through Jmjd3-dependent metabolic and epigenetic reprogramming and inactivates the M1 phenotype by silencing the NF- $\kappa$ B pathway via PHD-regulated proline hydroxylation of protein kinase IKK $\beta$  [283]. However, glutamine anaplerosis partially replenishes succinate to activate M1 macrophages [198, 282]. Recently, dietary glutamine supply in limb ischemia-bearing diabetic mice reduced the M1/M2 ratio to promote muscle regeneration [284]. Glutaminolysis-induced M2 polarization was identified as an underlying target for obesity and type2 diabetes [282]. Contrarily, blocking glutamine metabolism skewed the macrophage phenotype toward M1 to exert antitumor immunity [194, 285]. Li et al. [189] loaded PVP-coated AuNPs into MOFs to synthesize the metabolic modulator Au@ZIF-8 via a two-step method, which enhanced GS activity (detected by a GS kit) to upregulate glutamine, altered other metabolic pathways (e.g., the TCA cycle), and remarkably decreased TNF- $\alpha$  secretion (analyzed by RT-qPCR) in LPS-induced RAW 264.7 cells, and applied it to glutamine metabolism-mediated diseases.

The fate of serine metabolism on macrophage polarization was investigated and a novel mechanism was proposed by which serine deficiency stimulates the M1 phenotype and inhibits STAT6-mediated M2 polarization by activating p38-dependent JAK–STAT-1 axis [286], suggesting that serine metabolism may be an underlying target. A recent study showed that serine supports LPS-dependent IL-1 $\beta$

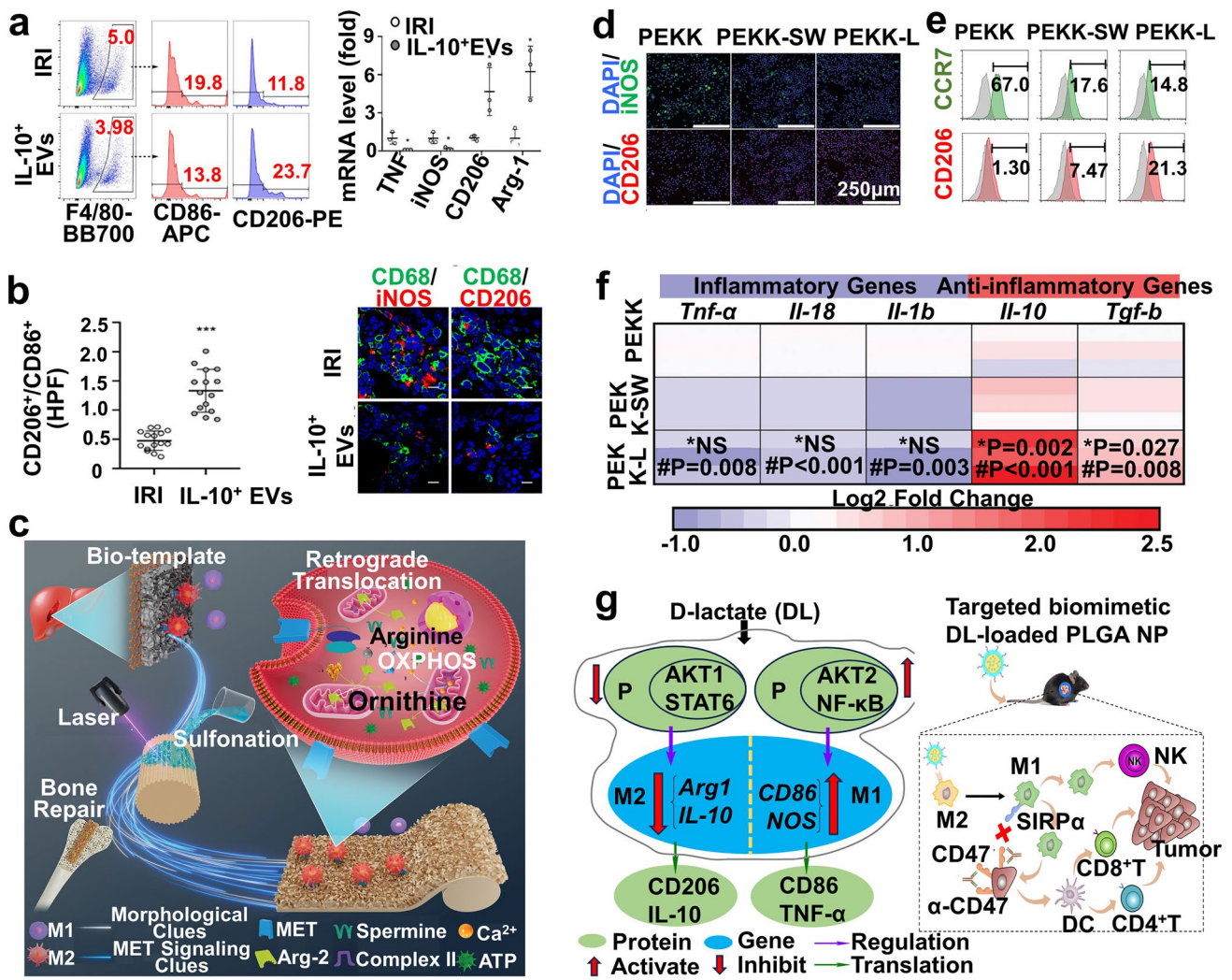


**Fig. 7** a, b IL-10<sup>+</sup> EVs promote macrophage M2 polarization [184]. Copyright 2020, American Association for the Advancement of Science. c Schematic of liver-inspired PEKK scaffolds that reprogram macrophage metabolism for increasing osteoporotic osseointegration. d, e IF staining and biomarker (CCR7 and CD206) expression by flow cytometry of RAW 264.7 cells cultured on various scaffolds. f A heatmap describing the fold-change in expressed polarization genes after treatment with different groups [190]. Copyright 2023, Wiley-VCH GmbH. g Possible mechanisms of DL-modulated TAM repolarization from M2 to M1 (left) and remodeling of the iTME for HCC therapy via DL delivery combined with α-CD47 (right) [195]. Copyright 2023, American Association for the Advancement of Science

production by synthesizing GSH in BMDMs and improving survival in a sepsis model by inhibiting de novo serine synthesis [287].

Considering the newly identified role of amino acid metabolism in macrophage polarization, we are optimistic that exploiting NMs to regulate amino acid metabolism within macrophages to emerge the desired phenotype will be a new research direction, although the blueprint is premature.

### 3.8 Lactate Metabolism

The metabolic adaptation of M1 macrophages leads to Warburg-type lactate accumulation [49]. Emerging evidence indicates that lactate serves as an immunomodulator [288] and mediates differentially expressed gene production [289], revealing that lactate may be the white swan of reshaping energy metabolism rather than a glycolytic “waste product.” Metabolites derived from nonimmune cells have been confirmed to affect the glycolysis–OXPHOS axis of immune cells and then reshape their phenotype [290]. Tumor

cell-derived lactate induces TAMs M2-related gene profiling in an HIF-1 $\alpha$ -dependent manner for promoting tumorigenesis [291–293]. This is somewhat confusing, and the accurate mechanism remains unclear, as the conventional view is that glycolysis with lactate accumulation supports M1, whereas OXPHOS responds to M2. A recent study by Zhao may explain the contradictory paradigm, which revealed that accumulated lactate in LPS(+IFN- $\gamma$ )-driven BMDMs serves as a precursor to stimulate histone lactylation at lysine residues (known as “K1a”). Increased histone K1a activates M2-like gene transcription via epigenetic modification [294].

Currently, the two conflicting methods of supplying D-lactate (DL) and depleting lactate manipulate macrophages toward the M1 phenotype for tumor immunotherapy. DL serves as an endogenous immunoregulator that enhances the phagocytic ability of Kupffer cells (a sign of M1 macrophages) [295]. Guo et al. [195] engineered biomimetic DL-loaded PLGA NPs and decorated them with a M2-binding peptide (M2pep)-modified hepatocellular carcinoma (HCC) membrane to prepare DL@NP-M-M2pep NPs (particle size ~ 120 nm) using an extruder. These NPs accumulated in tumors through HCC membrane-related homing ability and subsequently delivered DL into IL-4-induced BMDMs via the M2 peptide-targeting capacity. This delivery drove M2-to-M1 transition, as measured via RT-qPCR, IF, and flow cytometry, thus remodeling the iTME primarily by blocking PI3K/Akt signaling downstream and activating the NF- $\kappa$ B pathway for carcinogen-induced HCC mice therapy (Fig. 7g). The finding first confirms the regulatory function of DL on TAM polarization and provides a reference for following research in this field.

Depleting lactate through a compatible matrix-laden lactate oxidase (Lox) [296] or bacteria has become an alternative strategy against tumor [197, 297, 298]. Regarding Lox, Liu et al. [196] loaded Lox, syrosingopine, and Gd/CeO<sub>2</sub> into ZIF-8 to develop urchin-like catalysts with a size of 300 nm via a wet-chemical approach, effectively depleting intratumoral lactate by releasing Lox (detected by hippocampal analyzer and lactate kit), achieving glycometabolic reprogramming to activate the M1 response in IL-4-induced BMDMs for achieving HCC-bearing mouse immunotherapy. M1/M2 polarization was identified by RT-qPCR, IF, and ELISA. This metabolic remodeling strategy targeting lactate may open a promising avenue for tumor therapy, which can be expanded to other representative metabolites in the iTME. Conversely, our group [299] incorporated engineered

*Lactococcus lactis* (*L. lactis*) into a heparin-polyoxamer copolymer to prepare a living hydrogel delivery system (HP@LL\_VEGF), which steadily secreted lactate from *L. lactis* as a metabolic signal to remodel LPS + IFN- $\gamma$ -induced BMDMs toward M2-like, (confirmed by IF, CLSM, flow cytometry, RT-qPCR, and WB, thus ameliorating inflammation in streptozotocin-induced diabetic mice and accelerating wound healing.

Lactate consumption and DL replenishment are believed to support macrophage M2-to-M1 polarization against tumor growth. However, these two mainstream strategies are contradictory, and researchers have not accurately elucidated the regulatory mechanism by which designed NMs influence macrophage polarization by regulating lactate levels. Lactate serves not only as a byproduct of glycolysis but also as a factor driving M2 polarization via K1a-induced Arg-1 expression. Addressing how to selectively deplete or supply lactate to avoid side effects on other physiological cells or tissues may be a major issue for researchers to consider.

## 4 Conclusion and Perspectives

NM-based repurposing of macrophage metabolism holds considerable potential in various disease scenario. Here, we outline recent advances in the application of NM-based metabolic reprogramming, providing a partial blueprint and insights into macrophage metabolic immunotherapy. We believe that a deeper understanding of the interaction between metabolism, polarization, and NMs can greatly accelerate the exploration of next-generation NMs with optimal performance under the strategic collaboration of multiple disciplines. Nevertheless, thorough research is needed in the future to conquer remaining challenges that have not been addressed and bring engineered NMs into clinical applications. The following section introduces additional information on the key issues that need to be addressed and future research priorities, yielding insights for future research.

- (1) Engineering NMs with macrophage-targeting moieties (e.g., ligand) to enhance phagocytic uptake or bridging stimuli-triggered units may achieve personalized targeting [300, 301]. NMs confront a series of pathophysiological barriers during transport in vivo. Their complex surface interfaces inevitably interact with proteins and cells in blood and tissues, leading to performance

change and inevitable clearance by the immune system [300]. NMs are inevitably internalized by other macrophage subsets or adjacent cells even within the same tissue due to the ubiquitous distribution of cells, resulting in unintended off-target effects and immunogenicity. Establishing a biomimetic Trojan delivery system that accurately targets specific macrophages subsets remains a challenge before entering clinical research. The pathogenesis of metabolic diseases is extremely complex, involving multiple altered parameters. Restricted by suboptimal efficacy of a single target and limited target screening [302], the perspective should gradually shift from the doctrine of “one molecule, one target, one disease” to “all-in-one” NMs based on a multipronged strategy that synergistically modulates multiple metabolic targets in macrophages [175].

- (2) The exploration of theranostic NMs requires more rigorous consideration to devise programmable cargo transport strategies, demonstrating a diagnostic logic to determine cargo release time, followed by a therapeutic logic to program cargo release, to timely adjust the therapeutic schedule. More metabolic parameters, such as fumarate,  $\alpha$ -KG, GLUT1, glycolytic enzymes (e.g., PKM2, hexokinase, pyruvate dehydrogenase), FAS-associated enzymes (e.g., fatty acid synthase, acetyl-CoA carboxylase), and other amino acids (e.g., tryptophan, methionine), also undergo significant alteration in the metabolic adaptation of macrophages [24, 303–306] and can serve as theoretical targets for innovative therapies. These are beyond the scope of this review and have not been extensively explored yet. A combination of imaging technologies and metabolic events has enabled us to visualize and quantify macrophage behaviors. To accelerate clinical translation, clinically mature imaging techniques (e.g., MRI, CT) and FDA-approved materials (e.g., PEG) should be prioritized to exploit nanomedicines.
- (3) Most preclinical results originate from cell lines and animal models, and not humans. Metabolic profiles vary between them and humans, as is the behavior of NMs [307, 308]. Undoubtedly, human tissue models will be introduced into metabolic research to eliminate the long-standing dependence on traditional models [309], such as 3D organoids, which better mimic human organs [310]. Due to inappropriate assessment models, inadequate understanding of nano–bio-interactions, etc., current macrophage nanomedicines rarely achieve practical clinical translation [311], as evidenced by their limited commercialization. Long-term safe administration in humans is essential. The biodegradability, pharmacokinetics, and long-term

toxicity of NMs must be analyzed in detail. Perhaps we can explore intracellular behavior of internalized NMs utilizing computational toxicology, micro “organ on chip” devices, and high-throughput drug screening to establish pharmacokinetic–pharmacodynamic models for elucidating the toxicological pathway and therapeutic value. The minimum information reporting in bio–nano-experimental literature (MIRIBEL) standard should be followed for accelerating their clinical translation [312].

- (4) Precision nanomedicine may be the future research trend, aimed to tailor patient-personalized therapeutic regimens through various cutting-edge technologies based on individual differences, to minimize iatrogenic damage and medical costs and maximize patient benefits [313]. This strategy probably avoids an adverse drug response caused by a “one size fits all” treatment without considering patient heterogeneity [314]. Similar variability probably exists in simple NMs labeled with targeted fragments. Algorithms (e.g., artificial intelligence) may be imperative for implementing precision medicine, which contribute to patient classification and NM design, such as predicting optimal size, pharmacokinetics, and prescreening NMs for better patient compliance [315]. Some questions are raised frequently about precision medicine: Can we provide tailor-designed nanomedicines for each patient? Besides the complex clinical approval process of personalized nanomedicine customization, the limitations of its manufacturing technology and high-cost development are questions for the future.

Overall, although these strategies highlight the impressive preclinical potential of NM-based macrophage immunotherapy, very few have directly entered the clinical arena. This recognition has prompted some experts to raise provocative questions, hoping to transform the discipline from merely potential platforms to those enabling to provide positive clinical outcomes. Encouraged by the prominent progress already made, it could be expected that macrophage immuno-nanomedicines will eventually enter the clinic and market in the near future.

## 5 Statistical Analysis

Each experiment in the cited literature was independently repeated at least three times, and all quantitative data were expressed as mean  $\pm$  standard deviation ( $X \pm SD$ ). The sample size for all experiments met the requirements for statistical



analysis. Pairwise comparisons of consecutive variables were analyzed using a two-tailed Student's *t* test to determine statistical significance for normally distributed variables. Non-normally distributed variables were analyzed using nonparametric tests such as the Mann–Whitney U test (Wilcoxon rank sum test) or the Kruskal–Wallis H test followed by Dunn's multiple-comparison test. The chi-square test was employed to compare and analyze the statistical significance of categorical variables between two groups. For multiple comparisons of variables, one-way ANOVA followed by Tukey's post hoc test was conducted, and two-way ANOVA was used for analyses involving two independent variables. Statistical analyses were performed using GraphPad Prism 9.5 software, with a *P* value of <0.05 considered statistically significant. The confidence interval for all statistical tests was set at 95%.

With the help of multiple databases, we identified potential biomarkers of metabolic pathways using Progenesis QI software (Waters Corporation, Milford, USA) for metabolomics analysis. These databases include the Human Metabolome Database (HMDB, <http://hmdb.ca/>), Genomes (KEGG, <http://www.genome.jp/kegg/>), mzCloud (<https://www.mzcloud.org/>), and MBRole 2.0 (<http://csbg.cnb.csic.es/mbrole2/>). The metabolites were screened using a combination of multidimensional and one-dimensional analysis methods.

**Acknowledgements** This work was financially supported by the National Natural Science Foundation of China (Nos. 92168106 and 82222039).

#### Declarations

**Conflict of interest** The authors declare no interest conflict. They have no known competing financial interests or personal relationships that could have appeared to influence the work reported in this paper.

**Open Access** This article is licensed under a Creative Commons Attribution 4.0 International License, which permits use, sharing, adaptation, distribution and reproduction in any medium or format, as long as you give appropriate credit to the original author(s) and the source, provide a link to the Creative Commons licence, and indicate if changes were made. The images or other third party material in this article are included in the article's Creative Commons licence, unless indicated otherwise in a credit line to the material. If material is not included in the article's Creative Commons licence and your intended use is not permitted by statutory regulation or exceeds the permitted use, you will need to obtain permission directly from the copyright holder. To view a copy of this licence, visit <http://creativecommons.org/licenses/by/4.0/>.

## References

1. K. Sadtler, A. Singh, M.T. Wolf, X. Wang, D.M. Pardo et al., Design, clinical translation and immunological response of biomaterials in regenerative medicine. *Nat. Rev. Mater.* **1**, 16040–16056 (2016). <https://doi.org/10.1038/natrevmats.2016.40>
2. R. Sridharan, A.R. Cameron, D.J. Kelly, C.J. Kearney, F.J. O'Brien, Biomaterial based modulation of macrophage polarization: a review and suggested design principles. *Mater. Today* **18**(6), 313–325 (2015). <https://doi.org/10.1016/j.mat-tod.2015.01.019>
3. T.A. Wynn, A. Chawla, J.W. Pollard, Macrophage biology in development, homeostasis and disease. *Nature* **496**(7446), 445–455 (2013). <https://doi.org/10.1038/nature12034>
4. L. Parisi, E. Gini, D. Baci, M. Tremolati, M. Fanuli et al., Macrophage polarization in chronic inflammatory diseases: Killers or builders? *J. Immunol. Res.* **2018**, 8917804 (2018). <https://doi.org/10.1155/2018/8917804>
5. D.M. Mosser, J.P. Edwards, Exploring the full spectrum of macrophage activation. *Nat. Rev. Immunol.* **8**(12), 958–969 (2008). <https://doi.org/10.1038/nri2448>
6. A. Mantovani, A. Sica, S. Sozzani, P. Allavena, A. Vecchi et al., The chemokine system in diverse forms of macrophage activation and polarization. *Trends Immunol.* **25**(12), 677–686 (2004). <https://doi.org/10.1016/j.it.2004.09.015>
7. J.J. O'Shea, P.J. Murray, Cytokine signaling modules in inflammatory responses. *Immunity* **28**(4), 477–487 (2008). <https://doi.org/10.1016/j.immuni.2008.03.002>
8. A. Shapouri-Moghaddam, S. Mohammadian, H. Vazini, M. Taghadosi, S.A. Esmaeili et al., Macrophage plasticity, polarization, and function in health and disease. *J. Cell. Physiol.* **233**(9), 6425–6440 (2018). <https://doi.org/10.1002/jcp.26429>
9. S. Gordon, F.O. Martinez, Alternative activation of macrophages: mechanism and functions. *Immunity* **32**(5), 593–604 (2010). <https://doi.org/10.1016/j.immuni.2010.05.007>
10. W. Xu, X. Zhao, M.R. Daha, C. van Kooten, Reversible differentiation of pro- and anti-inflammatory macrophages. *Mol. Immunol.* **53**(3), 179–186 (2013). <https://doi.org/10.1016/j.molimm.2012.07.005>
11. E.L. Mills, B. Kelly, A. Logan, A.S.H. Costa, M. Varma et al., Succinate dehydrogenase supports metabolic repurposing of mitochondria to drive inflammatory macrophages. *Cell* **167**(2), 457–470.e413 (2016). <https://doi.org/10.1016/j.cell.2016.08.064>
12. D.G. Ryan, L.A.J. O'Neill, Krebs cycle reborn in macrophage immunometabolism. *Annu. Rev. Immunol.* **38**, 289–313 (2020). <https://doi.org/10.1146/annurev-immunol-081619-104850>
13. E.L. Mills, B. Kelly, L.A.J. O'Neill, Mitochondria are the powerhouses of immunity. *Nat. Immunol.* **18**(5), 488–498 (2017). <https://doi.org/10.1038/ni.3704>
14. J. Van den Bossche, L.A. O'Neill, D. Menon, Macrophage immunometabolism: where are we (going)? *Trends Immunol.* **38**(6), 395–406 (2017). <https://doi.org/10.1016/j.it.2017.03.001>

15. E.L. Mills, L.A. O'Neill, Reprogramming mitochondrial metabolism in macrophages as an anti-inflammatory signal. *Eur. J. Immunol.* **46**(1), 13–21 (2016). <https://doi.org/10.1002/eji.201445427>
16. A.K. Jha, S.C. Huang, A. Sergushichev, V. Lampropoulou, Y. Ivanova et al., Network integration of parallel metabolic and transcriptional data reveals metabolic modules that regulate macrophage polarization. *Immunity* **42**(3), 419–430 (2015). <https://doi.org/10.1016/j.immuni.2015.02.005>
17. A.M. Kabat, E.J. Pearce, Inflammation by way of macrophage metabolism. *Science* **356**(6337), 488–489 (2017). <https://doi.org/10.1126/science.aan2691>
18. I. Vitale, G. Manic, L.M. Coussens, G. Kroemer, L. Galluzzi, Macrophages and metabolism in the tumor microenvironment. *Cell Metab.* **30**(1), 36–50 (2019). <https://doi.org/10.1016/j.cmet.2019.06.001>
19. J. Li, X. Jiang, H. Li, M. Gelinsky, Z. Gu, Tailoring materials for modulation of macrophage fate. *Adv. Mater.* **33**(12), e2004172 (2021). <https://doi.org/10.1002/adma.202004172>
20. L. Zhang, X. Chen, P. Cai, H. Sun, S. Shen et al., Reprogramming mitochondrial metabolism in synovial macrophages of early osteoarthritis by a camouflaged meta-defensome. *Adv. Mater.* **34**(30), e2202715 (2022). <https://doi.org/10.1002/adma.202202715>
21. L. Wang, D. Wang, T. Zhang, Y. Ma, X. Tong et al., The role of immunometabolism in macrophage polarization and its impact on acute lung injury/acute respiratory distress syndrome. *Front. Immunol.* **14**, 1117548 (2023). <https://doi.org/10.3389/fimmu.2023.1117548>
22. S. Cai, M. Zhao, B. Zhou, A. Yoshii, D. Bugg et al., Mitochondrial dysfunction in macrophages promotes inflammation and suppresses repair after myocardial infarction. *J. Clin. Invest.* **133**(4), e159498 (2023). <https://doi.org/10.1172/JCI159498>
23. S.A. Eming, P.J. Murray, E.J. Pearce, Metabolic orchestration of the wound healing response. *Cell Metab.* **33**(9), 1726–1743 (2021). <https://doi.org/10.1016/j.cmet.2021.07.017>
24. A. Castegna, R. Gissi, A. Menga, M. Montopoli, M. Favia et al., Pharmacological targets of metabolism in disease: opportunities from macrophages. *Pharmacol. Ther.* **210**, 107521 (2020). <https://doi.org/10.1016/j.pharmthera.2020.107521>
25. P. Hou, J. Fang, Z. Liu, Y. Shi, M. Agostini et al., Macrophage polarization and metabolism in atherosclerosis. *Cell Death Dis.* **14**(10), 691 (2023). <https://doi.org/10.1038/s41419-023-06206-z>
26. W.K.E. Ip, N. Hoshi, D.S. Shouval, S. Snapper, R. Medzhitov, Anti-inflammatory effect of IL-10 mediated by metabolic reprogramming of macrophages. *Science* **356**(6337), 513–519 (2017). <https://doi.org/10.1126/science.aal3535>
27. R.A. Franklin, W. Liao, A. Sarkar, M.V. Kim, M.R. Bivona et al., The cellular and molecular origin of tumor-associated macrophages. *Science* **344**(6186), 921–925 (2014). <https://doi.org/10.1126/science.1252510>
28. M. Li, Y. Yang, L. Xiong, P. Jiang, J. Wang et al., Metabolism, metabolites, and macrophages in cancer. *J. Hematol. Oncol.* **16**(1), 80 (2023). <https://doi.org/10.1186/s13045-023-01478-6>
29. D. Kim, Y.W. Wu, Q.Y. Li, Y.K. Oh, Nanoparticle-mediated lipid metabolic reprogramming of T cells in tumor microenvironments for immunometabolic therapy. *Nano-Micro Lett.* **13**(1), 31 (2021). <https://doi.org/10.1007/s40820-020-00555-6>
30. T. Hou, T. Wang, W. Mu, R. Yang, S. Liang et al., Nanoparticle-loaded polarized-macrophages for enhanced tumor targeting and cell-chemotherapy. *Nano-Micro Lett.* **13**(1), 6 (2020). <https://doi.org/10.1007/s40820-020-00531-0>
31. J. Mao, L. Chen, Z. Cai, S. Qian, Z. Liu et al., Advanced biomaterials for regulating polarization of macrophages in wound healing. *Adv. Funct. Mater.* **32**(12), 2111003 (2021). <https://doi.org/10.1002/adfm.202111003>
32. E. Peled, A. Sosnik, Amphiphilic galactomannan nanoparticles trigger the alternative activation of murine macrophages. *J. Control. Release* **339**, 473–483 (2021). <https://doi.org/10.1016/j.jconrel.2021.10.017>
33. J. Tang, S. Baxter, A. Menon, A. Alaarg, B.L. Sanchez-Gaytan et al., Immune cell screening of a nanoparticle library improves atherosclerosis therapy. *Proc. Natl. Acad. Sci. U.S.A.* **113**(44), E6731–E6740 (2016). <https://doi.org/10.1073/pnas.1609629113>
34. H.J. Jeong, R.J. Yoo, J.K. Kim, M.H. Kim, S.H. Park et al., Macrophage cell tracking pet imaging using mesoporous silica nanoparticles via in vivo bioorthogonal F-18 labeling. *Biomaterials* **199**, 32–39 (2019). <https://doi.org/10.1016/j.biomaterials.2019.01.043>
35. S.B. Lee, H.W. Lee, T.D. Singh, Y. Li, S.K. Kim et al., Visualization of macrophage recruitment to inflammation lesions using highly sensitive and stable radionuclide-embedded gold nanoparticles as a nuclear bio-imaging platform. *Theranostics* **7**(4), 926–934 (2017). <https://doi.org/10.7150/thno.17131>
36. J. Toczek, P. Boodagh, N. Sanzida, M. Ghim, M. Salarian et al., Computed tomography imaging of macrophage phagocytic activity in abdominal aortic aneurysm. *Theranostics* **11**(12), 5876–5888 (2021). <https://doi.org/10.7150/thno.55106>
37. Z. Guo, L. Yang, M. Chen, X. Wen, H. Liu et al., Molecular imaging of advanced atherosclerotic plaques with folate receptor-targeted 2D nanoprobes. *Nano Res.* **13**(1), 173–182 (2019). <https://doi.org/10.1007/s12274-019-2592-4>
38. H. Deng, X. Li, J. Ju, X. Mo, G. Ge et al., Multifunctional nanoprobes for macrophage imaging. *Biomaterials* **290**, 121824 (2022). <https://doi.org/10.1016/j.biomaterials.2022.121824>
39. A. Ramesh, N. Deshpande, V. Malik, A. Nguyen, M. Malhotra et al., Activatable nanoreporters for real-time tracking of macrophage phenotypic states associated with disease progression. *Small* **19**(41), e2300978 (2023). <https://doi.org/10.1002/smll.202300978>
40. X. Liu, X. Xie, J. Jiang, M. Lin, E. Zheng et al., Use of nanoformulation to target macrophages for disease treatment.

- Adv. Funct. Mater. **31**(38), 2104487 (2021). <https://doi.org/10.1002/adfm.202104487>
41. Y. Zhu, S. Hideyoshi, H. Jiang, Y. Matsumura, J.L. Dziki et al., Injectable, porous, biohybrid hydrogels incorporating decellularized tissue components for soft tissue applications. *Acta Biomater.* **73**, 112–126 (2018). <https://doi.org/10.1016/j.actbio.2018.04.003>
  42. H. Yao, F. Wang, H. Chong, J. Wang, Y. Bai et al., A curcumin-modified coordination polymers with ROS scavenging and macrophage phenotype regulating properties for efficient ulcerative colitis treatment. *Adv. Sci.* **10**(19), e2300601 (2023). <https://doi.org/10.1002/advs.202300601>
  43. L. Hou, X. Gong, J. Yang, H. Zhang, W. Yang et al., Hybrid-membrane-decorated prussian blue for effective cancer immunotherapy via tumor-associated macrophages polarization and hypoxia relief. *Adv. Mater.* **34**(14), e2200389 (2022). <https://doi.org/10.1002/adma.202200389>
  44. P.K. Langston, M. Shibata, T. Horng, Metabolism supports macrophage activation. *Front. Immunol.* **8**, 61 (2017). <https://doi.org/10.3389/fimmu.2017.00061>
  45. D.E. Lackey, J.M. Olefsky, Regulation of metabolism by the innate immune system. *Nat. Rev. Endocrinol.* **12**(1), 15–28 (2016). <https://doi.org/10.1038/nrendo.2015.189>
  46. O. Osborn, J.M. Olefsky, The cellular and signaling networks linking the immune system and metabolism in disease. *Nat. Med.* **18**(3), 363–374 (2012). <https://doi.org/10.1038/nm.2627>
  47. G.J. Koelwyn, E.M. Corr, E. Erbay, K.J. Moore, Regulation of macrophage immunometabolism in atherosclerosis. *Nat. Immunol.* **19**(6), 526–537 (2018). <https://doi.org/10.1038/s41590-018-0113-3>
  48. V. Kumar, Targeting macrophage immunometabolism: dawn in the darkness of sepsis. *Int. Immunopharmacol.* **58**, 173–185 (2018). <https://doi.org/10.1016/j.intimp.2018.03.005>
  49. S. Galvan-Pena, L.A. O'Neill, Metabolic reprogramming in macrophage polarization. *Front. Immunol.* **5**, 420 (2014). <https://doi.org/10.3389/fimmu.2014.00420>
  50. M. Xie, Y. Yu, R. Kang, S. Zhu, L. Yang et al., PKM2-dependent glycolysis promotes NLRP3 and AIM2 inflammasome activation. *Nat. Commun.* **7**, 13280 (2016). <https://doi.org/10.1038/ncomms13280>
  51. E.M. Palsson-McDermott, A.M. Curtis, G. Goel, M.A.R. Lauterbach, F.J. Sheedy et al., Pyruvate kinase M2 regulates Hif-1alpha activity and IL-1beta induction and is a critical determinant of the warburg effect in LPS-activated macrophages. *Cell Metab.* **21**(2), 347 (2015). <https://doi.org/10.1016/j.cmet.2015.01.017>
  52. K. Mehla, P.K. Singh, Metabolic regulation of macrophage polarization in cancer. *Trends Cancer* **5**(12), 822–834 (2019). <https://doi.org/10.1016/j.trecan.2019.10.007>
  53. L.A. O'Neill, R.J. Kishton, J. Rathmell, A guide to immunometabolism for immunologists. *Nat. Rev. Immunol.* **16**(9), 553–565 (2016). <https://doi.org/10.1038/nri.2016.70>
  54. B.J. Altman, Z.E. Stine, C.V. Dang, From krebs to clinic: glutamine metabolism to cancer therapy. *Nat. Rev. Cancer* **16**(11), 749 (2016). <https://doi.org/10.1038/nrc.2016.114>
  55. M. Trauelsen, T.K. Hiron, D. Lin, J.E. Petersen, B. Breton et al., Extracellular succinate hyperpolarizes M2 macrophages through SUCNR1/GRP91-mediated gq signaling. *Cell Rep.* **35**(11), 109246 (2021). <https://doi.org/10.1016/j.celrep.2021.109246>
  56. M. de Castro Fonseca, C.J. Aguiar, J.A. da Rocha Franco, R.N. Gingold, M.F. Leite, GRP91: expanding the frontiers of Krebs cycle intermediates. *Cell Commun. Signal* **14**, 3 (2016). <https://doi.org/10.1186/s12964-016-0126-1>
  57. T. Reimann, D. Buscher, R.A. Hipskind, S. Krautwald, M.L. Lohmann-Matthes et al., Lipopolysaccharide induces activation of the Raf-1/MAP kinase pathway. A putative role for Raf-1 in the induction of the IL-1 beta and the TNF-alpha genes. *J. Immunol.* **153**(12), 5740–5749 (1994). <https://doi.org/10.4049/jimmunol.153.12.5740>
  58. M. Rath, I. Muller, P. Kropf, E.I. Closs, M. Munder, Metabolism via arginase or nitric oxide synthase: two competing arginine pathways in macrophages. *Front. Immunol.* **5**, 532 (2014). <https://doi.org/10.3389/fimmu.2014.00532>
  59. J.E. Qualls, C. Subramanian, W. Rafi, A.M. Smith, L. Balouzian et al., Sustained generation of nitric oxide and control of mycobacterial infection requires argininosuccinate synthase 1. *Cell Host Microbe* **12**(3), 313–323 (2012). <https://doi.org/10.1016/j.chom.2012.07.012>
  60. B. Beltran, A. Mathur, M.R. Duchon, J.D. Erusalimsky, S. Moncada, The effect of nitric oxide on cell respiration: a key to understanding its role in cell survival or death. *Proc. Natl. Acad. Sci. U.S.A.* **97**(26), 14602–14607 (2000). <https://doi.org/10.1073/pnas.97.26.14602>
  61. J. Van den Bossche, J. Baardman, N.A. Otto, S. van der Velden, A.E. Neele et al., Mitochondrial dysfunction prevents repolarization of inflammatory macrophages. *Cell Rep.* **17**(3), 684–696 (2016). <https://doi.org/10.1016/j.celrep.2016.09.008>
  62. E.L. Pearce, E.J. Pearce, Metabolic pathways in immune cell activation and quiescence. *Immunity* **38**(4), 633–643 (2013). <https://doi.org/10.1016/j.immuni.2013.04.005>
  63. M. Hesse, M. Modolell, A.C. La Flamme, M. Schito, J.M. Fuentes et al., Differential regulation of nitric oxide synthase-2 and arginase-1 by type 1/type 2 cytokines in vivo: granulomatous pathology is shaped by the pattern of L-arginine metabolism. *J. Immunol.* **167**(11), 6533–6544 (2001). <https://doi.org/10.4049/jimmunol.167.11.6533>
  64. J. Van den Bossche, W.H. Lamers, E.S. Koehler, J.M. Geuns, L. Alhonen et al., Pivotal advance: arginase-1-independent polyamine production stimulates the expression of IL-4-induced alternatively activated macrophage markers while inhibiting LPS-induced expression of inflammatory genes. *J. Leukoc. Biol.* **91**(5), 685–699 (2012). <https://doi.org/10.1189/jlb.0911453>
  65. N. Sukhbaatar, T. Weichhart, Iron regulation: macrophages in control. *Pharmaceuticals* **11**(4), 137 (2018). <https://doi.org/10.3390/ph11040137>

66. D.J. Kosman, Redox cycling in iron uptake, efflux, and trafficking. *J. Biol. Chem.* **285**(35), 26729–26735 (2010). <https://doi.org/10.1074/jbc.R110.113217>
67. M.P. Soares, I. Hamza, Macrophages and iron metabolism. *Immunity* **44**(3), 492–504 (2016). <https://doi.org/10.1016/j.immuni.2016.02.016>
68. E. Nemeth, M.S. Tuttle, J. Powelson, M.B. Vaughn, A. Donovan et al., Hepcidin regulates cellular iron efflux by binding to ferroportin and inducing its internalization. *Science* **306**(5704), 2090–2093 (2004). <https://doi.org/10.1126/science.1104742>
69. X.B. Liu, N.B. Nguyen, K.D. Marquess, F. Yang, D.J. Haile, Regulation of hepcidin and ferroportin expression by lipopolysaccharide in splenic macrophages. *Blood Cells Mol. Dis.* **35**(1), 47–56 (2005). <https://doi.org/10.1016/j.bcmd.2005.04.006>
70. G. Cairo, S. Recalcati, A. Mantovani, M. Locati, Iron trafficking and metabolism in macrophages: contribution to the polarized phenotype. *Trends Immunol.* **32**(6), 241–247 (2011). <https://doi.org/10.1016/j.it.2011.03.007>
71. M. Pereira, T.D. Chen, N. Buang, A. Olona, J.H. Ko et al., Acute iron deprivation reprograms human macrophage metabolism and reduces inflammation in vivo. *Cell Rep.* **28**(2), 498–511.e495 (2019). <https://doi.org/10.1016/j.celrep.2019.06.039>
72. A.B. Parekh, J.W. Putney Jr., Store-operated calcium channels. *Physiol. Rev.* **85**(2), 757–810 (2005). <https://doi.org/10.1152/physrev.00057.2003>
73. S. Feske, H. Wulff, E.Y. Skolnik, Ion channels in innate and adaptive immunity. *Annu. Rev. Immunol.* **33**, 291–353 (2015). <https://doi.org/10.1146/annurev-immunol-032414-112212>
74. C. Giorgi, S. Marchi, P. Pinton, The machineries, regulation and cellular functions of mitochondrial calcium. *Nat. Rev. Mol. Cell Biol.* **19**(11), 713–730 (2018). <https://doi.org/10.1038/s41580-018-0052-8>
75. P. He, F. Liu, M. Li, M. Ren, X. Wang et al., Mitochondrial calcium ion nanogluttons alleviate periodontitis via controlling mPTPs. *Adv. Healthc. Mater.* **12**(15), e2203106 (2023). <https://doi.org/10.1002/adhm.202203106>
76. O. Krenkel, F. Tacke, Liver macrophages in tissue homeostasis and disease. *Nat. Rev. Immunol.* **17**(5), 306–321 (2017). <https://doi.org/10.1038/nri.2017.11>
77. D. Vats, L. Mukundan, J.I. Odegaard, L. Zhang, K.L. Smith et al., Oxidative metabolism and PGC-1 $\beta$  attenuate macrophage-mediated inflammation. *Cell Metab.* **4**(1), 13–24 (2006). <https://doi.org/10.1016/j.cmet.2006.05.011>
78. J.T. Hou, K.K. Yu, K. Sunwoo, W.Y. Kim, S. Koo et al., Fluorescent imaging of reactive oxygen and nitrogen species associated with pathophysiological processes. *Chem* **6**(4), 832–866 (2020). <https://doi.org/10.1016/j.chempr.2019.12.005>
79. L.A. O'Neill, E.J. Pearce, Immunometabolism governs dendritic cell and macrophage function. *J. Exp. Med.* **213**(1), 15–23 (2016). <https://doi.org/10.1084/jem.20151570>
80. E. Rendra, V. Riabov, D.M. Mossel, T. Sevastyanova, M.C. Harmsen et al., Reactive oxygen species (ROS) in macrophage activation and function in diabetes. *Immunobiology* **224**(2), 242–253 (2019). <https://doi.org/10.1016/j.imbio.2018.11.010>
81. L. Formentini, F. Santacatterina, C. Nunez de Arenas, K. Stamatakis, D. Lopez-Martinez et al., Mitochondrial ROS production protects the intestine from inflammation through functional M2 macrophage polarization. *Cell Rep.* **19**(6), 1202–1213 (2017). <https://doi.org/10.1016/j.celrep.2017.04.036>
82. A.P. West, I.E. Brodsky, C. Rahner, D.K. Woo, H. Erdjument-Bromage et al., TLR signalling augments macrophage bactericidal activity through mitochondrial ROS. *Nature* **472**(7344), 476–480 (2011). <https://doi.org/10.1038/nature09973>
83. M. Hori, K. Nishida, Oxidative stress and left ventricular remodelling after myocardial infarction. *Cardiovasc. Res.* **81**(3), 457–464 (2009). <https://doi.org/10.1093/cvr/cvn335>
84. X. Li, Y. Liu, X. Qi, S. Xiao, Z. Xu et al., Sensitive activatable nanoprobes for real-time ratiometric magnetic resonance imaging of reactive oxygen species and ameliorating inflammation in vivo. *Adv. Mater.* **34**(19), e2109004 (2022). <https://doi.org/10.1002/adma.202109004>
85. B.X. Ma, H. Xu, W.H. Zhuang, Y.N. Wang, G.C. Li et al., Reactive oxygen species responsive theranostic nanoplatfor for two-photon aggregation-induced emission imaging and therapy of acute and chronic inflammation. *ACS Nano* **14**(5), 5862–5873 (2020). <https://doi.org/10.1021/acsnano.0c01012>
86. H. Wang, D. Yu, B. Li, Z. Liu, J. Ren et al., Ultrasensitive magnetic resonance imaging of systemic reactive oxygen species in vivo for early diagnosis of sepsis using activatable nanoprobes. *Chem. Sci.* **10**(13), 3770–3778 (2019). <https://doi.org/10.1039/c8sc04961k>
87. B.A. Berkowitz, Oxidative stress measured in vivo without an exogenous contrast agent using quest MRI. *J. Magn. Reson.* **291**, 94–100 (2018). <https://doi.org/10.1016/j.jmr.2018.01.013>
88. E.M. Espinoza, J.J. Roise, I.C. Li, R. Das, N. Murthy, Advances in imaging reactive oxygen species. *J. Nucl. Med.* **62**(4), 457–461 (2021). <https://doi.org/10.2967/jnumed.120.245415>
89. B.J. Crielard, C.J. Rijcken, L. Quan, S. van der Wal, I. Altintas et al., Glucocorticoid-loaded core-cross-linked polymeric micelles with tailorable release kinetics for targeted therapy of rheumatoid arthritis. *Angew. Chem. Int. Ed.* **51**(29), 7254–7258 (2012). <https://doi.org/10.1002/anie.201202713>
90. G. Yang, M. Fan, J. Zhu, C. Ling, L. Wu et al., A multifunctional anti-inflammatory drug that can specifically target activated macrophages, massively deplete intracellular H<sub>2</sub>O<sub>2</sub>, and produce large amounts CO for a highly efficient treatment of osteoarthritis. *Biomaterials* **255**, 120155 (2020). <https://doi.org/10.1016/j.biomaterials.2020.120155>
91. A. Bellahcene, M.J. Nokin, V. Castronovo, C. Schalkwijk, Methylglyoxal-derived stress: an emerging biological factor involved in the onset and progression of cancer. *Semin.*



- Cancer Biol. **49**, 64–74 (2018). <https://doi.org/10.1016/j.semcancer.2017.05.010>
92. Z. Mao, M. Ye, W. Hu, X. Ye, Y. Wang et al., Design of a ratiometric two-photon probe for imaging of hypochlorous acid (HClO) in wounded tissues. *Chem. Sci.* **9**(28), 6035–6040 (2018). <https://doi.org/10.1039/c8sc01697f>
93. M. Yao, Y. Lu, L. Shi, Y. Huang, Q. Zhang et al., A ROS-responsive, self-immolative and self-reporting hydrogen sulfide donor with multiple biological activities for the treatment of myocardial infarction. *Bioact. Mater.* **9**, 168–182 (2022). <https://doi.org/10.1016/j.bioactmat.2021.07.011>
94. H. Feng, Z. Zhang, Q. Meng, H. Jia, Y. Wang et al., Rapid response fluorescence probe enabled in vivo diagnosis and assessing treatment response of hypochlorous acid-mediated rheumatoid arthritis. *Adv. Sci.* **5**(8), 1800397 (2018). <https://doi.org/10.1002/advs.201800397>
95. R. Zhang, J. Zhao, G. Han, Z. Liu, C. Liu et al., Real-time discrimination and versatile profiling of spontaneous reactive oxygen species in living organisms with a single fluorescent probe. *J. Am. Chem. Soc.* **138**(11), 3769–3778 (2016). <https://doi.org/10.1021/jacs.5b12848>
96. C. Zhao, Z. Li, J. Chen, L. Su, J. Wang et al., Site-specific biomimicry of antioxidative melanin formation and its application for acute liver injury therapy and imaging. *Adv. Mater.* **33**(34), e2102391 (2021). <https://doi.org/10.1002/adma.202102391>
97. C. Zhao, J. Chen, J. Ye, Z. Li, L. Su et al., Structural transformative antioxidants for dual-responsive anti-inflammatory delivery and photoacoustic inflammation imaging. *Angew. Chem. Int. Ed.* **60**(26), 14458–14466 (2021). <https://doi.org/10.1002/anie.202100873>
98. X. Ai, Z. Wang, H. Cheong, Y. Wang, R. Zhang et al., Multi-spectral optoacoustic imaging of dynamic redox correlation and pathophysiological progression utilizing upconversion nanoprobes. *Nat. Commun.* **10**(1), 1087 (2019). <https://doi.org/10.1038/s41467-019-09001-7>
99. Z. Lei, F. Zhang, Molecular engineering of NIR-II fluorophores for improved biomedical detection. *Angew. Chem. Int. Ed.* **60**(30), 16294–16308 (2021). <https://doi.org/10.1002/anie.202007040>
100. C. Chu, J. Yu, E. Ren, S. Ou, Y. Zhang et al., Multimodal photoacoustic imaging-guided regression of corneal neovascularization: a non-invasive and safe strategy. *Adv. Sci.* **7**(14), 2000346 (2020). <https://doi.org/10.1002/advs.202000346>
101. Y. Ni, H. Liu, D. Dai, X. Mu, J. Xu et al., Chromogenic, fluorescent, and redox sensors for multichannel imaging and detection of hydrogen peroxide in living cell systems. *Anal. Chem.* **90**(17), 10152–10158 (2018). <https://doi.org/10.1021/acs.analchem.7b04435>
102. R. Singh, W. Zhang, X. Liu, B. Zhang, S. Kumar, Waveflex biosensor: MXene-Immobilized W-shaped fiber-based LSPR sensor for highly selective tyramine detection. *Opt. Laser Technol.* **171**, 110357 (2024). <https://doi.org/10.1016/j.optla.2023.110357>
103. H.C. Gomes, X. Liu, A. Fernandes, C. Moreirinha, R. Singh et al., Laser-induced graphene-based Fabry-Pérot cavity label-free immunosensors for the quantification of cortisol. *Sens. Actuators Rep.* **7**, 100186 (2024). <https://doi.org/10.1016/j.snr.2024.100186>
104. R. Singh, W. Zhang, X. Liu, B. Zhang, S. Kumar, Humanoid-shaped waveflex biosensor for the detection of food contamination. *Biomed. Opt. Express* **14**(9), 4660–4676 (2023). <https://doi.org/10.1364/boe.500311>
105. G. Zhang, R. Singh, B. Zhang, S. Kumar, G. Li, Waveflex biosensor based on S-tapered and waist-expanded technique for detection of glycosylated hemoglobin. *Biomed. Opt. Express* **14**(11), 6100–6113 (2023). <https://doi.org/10.1364/boe.505864>
106. G. Li, X. Li, R. Singh, G. Zhang, B. Zhang et al., Slide-type waveflex biosensor based on signal enhancement technology for alpha-fetoprotein detection. *Opt. Lett.* **48**(18), 4745–4748 (2023). <https://doi.org/10.1364/OL.501864>
107. R. Singh, S. Kumar, S. Bera, S.K. Bhunia, Trends in using fluorescent mxene quantum dots for selective detection and bioimaging applications: a review. *ACS Appl. Nano Mater.* **6**(21), 19526–19550 (2023). <https://doi.org/10.1021/acsnm.3c04491>
108. R. Singh, Z. Wang, C. Marques, R. Min, B. Zhang et al., Alanine aminotransferase detection using TIT assisted four tapered fiber structure-based LSPR sensor: from healthcare to marine life. *Biosens. Bioelectron.* **236**, 115424 (2023). <https://doi.org/10.1016/j.bios.2023.115424>
109. A.M. Cameron, A. Castoldi, D.E. Sanin, L.J. Flachsmann, C.S. Field et al., Inflammatory macrophage dependence on NAD(+) salvage is a consequence of reactive oxygen species-mediated DNA damage. *Nat. Immunol.* **20**(4), 420–432 (2019). <https://doi.org/10.1038/s41590-019-0336-y>
110. R.M. Palmer, A.G. Ferrige, S. Moncada, Nitric oxide release accounts for the biological activity of endothelium-derived relaxing factor. *Nature* **327**(6122), 524–526 (1987). <https://doi.org/10.1038/327524a0>
111. E. Sasaki, H. Kojima, H. Nishimatsu, Y. Urano, K. Kikuchi et al., Highly sensitive near-infrared fluorescent probes for nitric oxide and their application to isolated organs. *J. Am. Chem. Soc.* **127**(11), 3684–3685 (2005). <https://doi.org/10.1021/ja042967z>
112. Y. Gabe, Y. Urano, K. Kikuchi, H. Kojima, T. Nagano, Highly sensitive fluorescence probes for nitric oxide based on boron dipyrromethene chromophore-rational design of potentially useful bioimaging fluorescence probe. *J. Am. Chem. Soc.* **126**(10), 3357–3367 (2004). <https://doi.org/10.1021/ja037944j>
113. H. Kojima, Y. Urano, K. Kikuchi, T. Higuchi, Y. Hirata et al., Fluorescent indicators for imaging nitric oxide production. *Angew. Chem. Int. Ed.* **38**(21), 3209–3212 (1999). [https://doi.org/10.1002/\(sici\)1521-3773\(19991102\)38:21%3c3209::aid-anie3209%3e3.0.co;2-6](https://doi.org/10.1002/(sici)1521-3773(19991102)38:21%3c3209::aid-anie3209%3e3.0.co;2-6)
114. M.M. Sadek, M.B.A. Olia, C.J. Nowell, N. Barlow, C.H. Schiesser et al., Characterisation of a novel coumarin-based fluorescent probe for monitoring nitric oxide production in macrophages. *Bioorgan. Med. Chem.* **25**(20), 5743–5748 (2017). <https://doi.org/10.1016/j.bmc.2017.08.054>

115. E.Y. Zhou, H.J. Knox, C.J. Reinhardt, G. Partipilo, M.J. Nilges et al., Near-infrared photoactivatable nitric oxide donors with integrated photoacoustic monitoring. *J. Am. Chem. Soc.* **140**(37), 11686–11697 (2018). <https://doi.org/10.1021/jacs.8b05514>
116. Z. Mao, H. Jiang, Z. Li, C. Zhong, W. Zhang et al., An N-nitrosation reactivity-based two-photon fluorescent probe for the specific in situ detection of nitric oxide. *Chem. Sci.* **8**(6), 4533–4538 (2017). <https://doi.org/10.1039/c7sc00416h>
117. J. Miao, Y. Huo, Q. Liu, Z. Li, H. Shi et al., A new class of fast-response and highly selective fluorescent probes for visualizing peroxynitrite in live cells, subcellular organelles, and kidney tissue of diabetic rats. *Biomaterials* **107**, 33–43 (2016). <https://doi.org/10.1016/j.biomaterials.2016.08.032>
118. Y. Huo, J. Miao, Y. Li, Y. Shi, H. Shi et al., Aromatic primary monoamine-based fast-response and highly specific fluorescent probes for imaging the biological signaling molecule nitric oxide in living cells and organisms. *J. Mater. Chem. B* **5**(13), 2483–2490 (2017). <https://doi.org/10.1039/c6tb03382b>
119. T.W. Shiu, Y.H. Chen, C.M. Wu, G. Singh, H.Y. Chen et al., Nitric oxide turn-on fluorescent probe based on deamination of aromatic primary monoamines. *Inorg. Chem.* **51**(9), 5400–5408 (2012). <https://doi.org/10.1021/ic300379u>
120. A. Fernandez, M. Vendrell, Smart fluorescent probes for imaging macrophage activity. *Chem. Soc. Rev.* **45**(5), 1182–1196 (2016). <https://doi.org/10.1039/c5cs00567a>
121. P. Yuan, X. Xu, D. Hu, Y. Chen, J. Fan et al., Highly sensitive imaging of tumor metastasis based on the targeting and polarization of M2-like macrophages. *J. Am. Chem. Soc.* **145**(14), 7941–7951 (2023). <https://doi.org/10.1021/jacs.2c13218>
122. Y. Huo, J. Miao, J. Fang, H. Shi, J. Wang et al., Aromatic secondary amine-functionalized fluorescent NO probes: improved detection sensitivity for NO and potential applications in cancer immunotherapy studies. *Chem. Sci.* **10**(1), 145–152 (2019). <https://doi.org/10.1039/c8sc03694b>
123. A. Ramesh, S. Kumar, A. Brouillard, D. Nandi, A. Kulkarni, A nitric oxide (NO) nanoreporter for noninvasive real-time imaging of macrophage immunotherapy. *Adv. Mater.* **32**(24), e2000648 (2020). <https://doi.org/10.1002/adma.202000648>
124. R. Radi, Peroxynitrite, a stealthy biological oxidant. *J. Biol. Chem.* **288**(37), 26464–26472 (2013). <https://doi.org/10.1074/jbc.R113.472936>
125. J. Kim, J. Park, H. Lee, Y. Choi, Y. Kim, A boronate-based fluorescent probe for the selective detection of cellular peroxynitrite. *Chem. Commun.* **50**(66), 9353–9356 (2014). <https://doi.org/10.1039/c4cc02943g>
126. J. Peng, A. Samanta, X. Zeng, S. Han, L. Wang et al., Real-time in vivo hepatotoxicity monitoring through chromophore-conjugated photon-upconverting nanoprobes. *Angew. Chem. Int. Ed.* **56**(15), 4165–4169 (2017). <https://doi.org/10.1002/anie.201612020>
127. C. Wang, W. Fan, Z. Zhang, Y. Wen, L. Xiong et al., Advanced nanotechnology leading the way to multimodal imaging-guided precision surgical therapy. *Adv. Mater.* **31**(49), e1904329 (2019). <https://doi.org/10.1002/adma.201904329>
128. L. Wu, Y. Ishigaki, W. Zeng, T. Harimoto, B. Yin et al., Generation of hydroxyl radical-activatable ratiometric near-infrared bimodal probes for early monitoring of tumor response to therapy. *Nat. Commun.* **12**(1), 6145 (2021). <https://doi.org/10.1038/s41467-021-26380-y>
129. Y. Wang, Y. Zhang, Z. Wang, J. Zhang, R.R. Qiao et al., Optical/MRI dual-modality imaging of M1 macrophage polarization in atherosclerotic plaque with macro-targeted upconversion luminescence probe. *Biomaterials* **219**, 119378 (2019). <https://doi.org/10.1016/j.biomaterials.2019.119378>
130. L. Yuan, W. Lin, Y. Yang, H. Chen, A unique class of near-infrared functional fluorescent dyes with carboxylic-acid-modulated fluorescence ON/OFF switching: rational design, synthesis, optical properties, theoretical calculations, and applications for fluorescence imaging in living animals. *J. Am. Chem. Soc.* **134**(2), 1200–1211 (2012). <https://doi.org/10.1021/ja209292b>
131. M. Schieber, N.S. Chandel, ROS function in redox signaling and oxidative stress. *Curr. Biol.* **24**(10), R453–R462 (2014). <https://doi.org/10.1016/j.cub.2014.03.034>
132. G. Morris, M. Gevezova, V. Sarafian, M. Maes, Redox regulation of the immune response. *Cell. Mol. Immunol.* **19**(10), 1079–1101 (2022). <https://doi.org/10.1038/s41423-022-00902-0>
133. J.S. Arthur, S.C. Ley, Mitogen-activated protein kinases in innate immunity. *Nat. Rev. Immunol.* **13**(9), 679–692 (2013). <https://doi.org/10.1038/nri3495>
134. H. Kamata, S. Honda, S. Maeda, L.F. Chang, H. Hirata et al., Reactive oxygen species promote TNF $\alpha$ -induced death and sustained JNK activation by inhibiting MAP kinase phosphatases. *Cell* **120**(5), 649–661 (2005). <https://doi.org/10.1016/j.cell.2004.12.041>
135. C. Wu, W. Zhao, X. Zhang, X. Chen, Neocryptotanshinone inhibits lipopolysaccharide-induced inflammation in RAW 264.7 macrophages by suppression of NF-kappaB and iNOS signaling pathways. *Acta. Pharm. Sin. B* **5**(4), 323–329 (2015). <https://doi.org/10.1016/j.apsb.2015.01.010>
136. C. Bogdan, Nitric oxide and the immune response. *Nat. Immunol.* **2**(10), 907–916 (2001). <https://doi.org/10.1038/ni1001-907>
137. V. Toshchakov, B.W. Jones, P.Y. Perera, K. Thomas, M.J. Cody et al., TLR4, but not TLR2, mediates IFN-beta-induced STAT1alpha/beta-dependent gene expression in macrophages. *Nat. Immunol.* **3**(4), 392–398 (2002). <https://doi.org/10.1038/ni774>
138. J.S. Ma, W.J. Kim, J.J. Kim, T.J. Kim, S.K. Ye et al., Gold nanoparticles attenuate LPS-induced NO production through the inhibition of NF-kappab and IFN-beta/STAT1 pathways in RAW264.7 cells. *Nitric Oxide* **23**(3), 214–219 (2010). <https://doi.org/10.1016/j.niox.2010.06.005>
139. E. Butturini, D. Boriero, A. Carcereri de Prati, S. Mariotto, STAT1 drives M1 microglia activation and



- neuroinflammation under hypoxia. *Arch. Biochem. Biophys.* **669**, 22–30 (2019). <https://doi.org/10.1016/j.abb.2019.05.011>
140. B. Everts, E. Amiel, G.J. van der Windt, T.C. Freitas, R. Chott et al., Commitment to glycolysis sustains survival of NO-producing inflammatory dendritic cells. *Blood* **120**(7), 1422–1431 (2012). <https://doi.org/10.1182/blood-2012-03-419747>
141. Q. Zhang, D. Dehaini, Y. Zhang, J. Zhou, X. Chen et al., Neutrophil membrane-coated nanoparticles inhibit synovial inflammation and alleviate joint damage in inflammatory arthritis. *Nat. Nanotechnol.* **13**(12), 1182–1190 (2018). <https://doi.org/10.1038/s41565-018-0254-4>
142. W. Yang, Y. Tao, Y. Wu, X. Zhao, W. Ye et al., Neutrophils promote the development of reparative macrophages mediated by ROS to orchestrate liver repair. *Nat. Commun.* **10**(1), 1076 (2019). <https://doi.org/10.1038/s41467-019-09046-8>
143. A. Gombozhapova, Y. Rogovskaya, V. Shurupov, M. Rebenkova, J. Kzyshkowska et al., Macrophage activation and polarization in post-infarction cardiac remodeling. *J. Biomed. Sci.* **24**(1), 13 (2017). <https://doi.org/10.1186/s12929-017-0322-3>
144. E.H. Choo, J.H. Lee, E.H. Park, H.E. Park, N.C. Jung et al., Infarcted myocardium-primed dendritic cells improve remodeling and cardiac function after myocardial infarction by modulating the regulatory T cell and macrophage polarization. *Circulation* **135**(15), 1444–1457 (2017). <https://doi.org/10.1161/CIRCULATIONAHA.116.023106>
145. Y. Liu, K. Ai, X. Ji, D. Askhatova, R. Du et al., Comprehensive insights into the multi-antioxidative mechanisms of melanin nanoparticles and their application to protect brain from injury in ischemic stroke. *J. Am. Chem. Soc.* **139**(2), 856–862 (2017). <https://doi.org/10.1021/jacs.6b11013>
146. X. Bao, J. Zhao, J. Sun, M. Hu, X. Yang, Polydopamine nanoparticles as efficient scavengers for reactive oxygen species in periodontal disease. *ACS Nano* **12**(9), 8882–8892 (2018). <https://doi.org/10.1021/acs.nano.8b04022>
147. C. Zhang, X. Wang, J. Du, Z. Gu, Y. Zhao, Reactive oxygen species-regulating strategies based on nanomaterials for disease treatment. *Adv. Sci.* **8**(3), 2002797 (2021). <https://doi.org/10.1002/advs.202002797>
148. L. Zhang, Q.C. Yang, S. Wang, Y. Xiao, S.C. Wan et al., Engineering multienzyme-mimicking covalent organic frameworks as pyroptosis inducers for boosting antitumor immunity. *Adv. Mater.* **34**(13), e2108174 (2022). <https://doi.org/10.1002/adma.202108174>
149. J. Zhang, B. Gao, B. Ye, Z. Sun, Z. Qian et al., Mitochondrial-targeted delivery of polyphenol-mediated antioxidant complexes against pyroptosis and inflammatory diseases. *Adv. Mater.* **35**(11), e2208571 (2023). <https://doi.org/10.1002/adma.202208571>
150. T. Liu, B. Xiao, F. Xiang, J. Tan, Z. Chen et al., Ultrasmall copper-based nanoparticles for reactive oxygen species scavenging and alleviation of inflammation related diseases. *Nat. Commun.* **11**(1), 2788 (2020). <https://doi.org/10.1038/s41467-020-16544-7>
151. Y. Peng, D. He, X. Ge, Y. Lu, Y. Chai et al., Construction of heparin-based hydrogel incorporated with Cu<sub>5</sub>4O ultrasmall nanozymes for wound healing and inflammation inhibition. *Bioact. Mater.* **6**(10), 3109–3124 (2021). <https://doi.org/10.1016/j.bioactmat.2021.02.006>
152. M. Soh, D.W. Kang, H.G. Jeong, D. Kim, D.Y. Kim et al., Ceria-Zirconia nanoparticles as an enhanced multi-antioxidant for sepsis treatment. *Angew. Chem. Int. Ed.* **56**(38), 11399–11403 (2017). <https://doi.org/10.1002/anie.201704904>
153. S.I. Han, S.W. Lee, M.G. Cho, J.M. Yoo, M.H. Oh et al., Epitaxially strained CeO<sub>2</sub>/Mn<sub>3</sub>O<sub>4</sub> nanocrystals as an enhanced antioxidant for radioprotection. *Adv. Mater.* **32**(31), e2001566 (2020). <https://doi.org/10.1002/adma.202001566>
154. X. Zhou, Q. Zhou, Z. He, Y. Xiao, Y. Liu et al., ROS balance autoregulating core-shell CeO<sub>2</sub>@ZIF-8/Au nanoplatform for wound repair. *Nano-Micro Lett.* **16**(1), 156 (2024). <https://doi.org/10.1007/s40820-024-01353-0>
155. J. Kim, H.Y. Kim, S.Y. Song, S.H. Go, H.S. Sohn et al., Synergistic oxygen generation and reactive oxygen species scavenging by manganese ferrite/ceria co-decorated nanoparticles for rheumatoid arthritis treatment. *ACS Nano* **13**(3), 3206–3217 (2019). <https://doi.org/10.1021/acs.nano.8b08785>
156. J. Mu, C. Li, Y. Shi, G. Liu, J. Zou et al., Protective effect of platinum nano-antioxidant and nitric oxide against hepatic ischemia-reperfusion injury. *Nat. Commun.* **13**(1), 2513 (2022). <https://doi.org/10.1038/s41467-022-29772-w>
157. X.D. Zhang, X.K. Chen, Y.L. Zhao, Nanozymes: versatile platforms for cancer diagnosis and therapy. *Nano-Micro Lett.* **14**(1), 95 (2022). <https://doi.org/10.1007/s40820-022-00828-2>
158. Y.J. Li, S.J.Y. Gao, S.R. Shi, D.X. Xiao, S.L. Peng et al., Tetrahedral framework nucleic acid-based delivery of resveratrol alleviates insulin resistance: from innate to adaptive immunity. *Nano-Micro Lett.* **13**(1), 186 (2021). <https://doi.org/10.1007/s40820-021-00711-6>
159. F. Zhou, M. Li, M. Chen, M. Chen, X. Chen et al., Redox homeostasis strategy for inflammatory macrophage reprogramming in rheumatoid arthritis based on ceria oxide nanozyme-complexed biopolymeric micelles. *ACS Nano* **17**(5), 4358–4372 (2023). <https://doi.org/10.1021/acs.nano.2c09127>
160. Y. Guo, Q. Sun, F.G. Wu, Y. Dai, X. Chen, Polyphenol-containing nanoparticles: synthesis, properties, and therapeutic delivery. *Adv. Mater.* **33**(22), e2007356 (2021). <https://doi.org/10.1002/adma.202007356>
161. M.S. Petronek, J.M. Stolwijk, S.D. Murray, E.J. Steinbach, Y. Zakharia et al., Utilization of redox modulating small molecules that selectively act as pro-oxidants in cancer cells to open a therapeutic window for improving cancer therapy. *Redox Biol.* **42**, 101864 (2021). <https://doi.org/10.1016/j.redox.2021.101864>
162. W.L. Wan, Y.J. Lin, H.L. Chen, C.C. Huang, P.C. Shih et al., In situ nanoreactor for photosynthesizing H<sub>2</sub> gas to mitigate oxidative stress in tissue inflammation. *J. Am. Chem. Soc.* **139**(37), 12923–12926 (2017). <https://doi.org/10.1021/jacs.7b07492>

163. B. Zhao, L. Zeng, D. Chen, S. Xie, Z. Jin et al., NIR-photocatalytic regulation of arthritic synovial microenvironment. *Sci. Adv.* **8**(40), eabq0959 (2022). <https://doi.org/10.1126/sciadv.abq0959>
164. G. Yang, J.S. Ni, Y. Li, M. Zha, Y. Tu et al., Acceptor engineering for optimized ROS generation facilitates reprogramming macrophages to M1 phenotype in photodynamic immunotherapy. *Angew. Chem. Int. Ed.* **60**(10), 5386–5393 (2021). <https://doi.org/10.1002/anie.202013228>
165. M.W. Cleeter, J.M. Cooper, V.M. Darley-Usmar, S. Moncada, A.H. Schapira, Reversible inhibition of cytochrome c oxidase, the terminal enzyme of the mitochondrial respiratory chain, by nitric oxide. Implications for neurodegenerative diseases. *FEBS Lett.* **345**(1), 50–54 (1994). [https://doi.org/10.1016/0014-5793\(94\)00424-2](https://doi.org/10.1016/0014-5793(94)00424-2)
166. S. Theivendran, Z. Gu, J. Tang, Y. Yang, H. Song et al., Nanostructured organosilica nitric oxide donors intrinsically regulate macrophage polarization with antitumor effect. *ACS Nano* **16**(7), 10943–10957 (2022). <https://doi.org/10.1021/acsnano.2c03348>
167. M. Liang, X. Yan, Nanozymes: from new concepts, mechanisms, and standards to applications. *Acc. Chem. Res.* **52**(8), 2190–2200 (2019). <https://doi.org/10.1021/acs.accounts.9b00140>
168. K. Sridhar, B.S. Inbaraj, B.H. Chen, Recent advances on nanoparticle based strategies for improving carotenoid stability and biological activity. *Antioxidants* **10**(5), 713 (2021). <https://doi.org/10.3390/antiox10050713>
169. D. Zhong, Z. Du, M. Zhou, Algae: a natural active material for biomedical applications. *View* **2**(4), 20200189 (2021). <https://doi.org/10.1002/viw.20200189>
170. H. Chen, Y. Guo, Z. Zhang, W. Mao, C. Shen et al., Symbiotic algae-bacteria dressing for producing hydrogen to accelerate diabetic wound healing. *Nano Lett.* **22**(1), 229–237 (2022). <https://doi.org/10.1021/acs.nanolett.1c03693>
171. W. Geng, X. Liu, B. Tao, Y. He, K. Li et al., Nitric oxide scavenging and hydrogen sulfide production synergistically treat rheumatoid arthritis. *Adv. Healthc. Mater.* **12**(4), 2202380 (2023). <https://doi.org/10.1002/adhm.202202380>
172. Y. Yan, A. Lu, Y. Dou, Z. Zhang, X.Y. Wang et al., Nanomedicines reprogram synovial macrophages by scavenging nitric oxide and silencing CA9 in progressive osteoarthritis. *Adv. Sci.* **10**(11), 2207490 (2023). <https://doi.org/10.1002/advs.202207490>
173. F. Zhou, J. Mei, S. Yang, X. Han, H. Li et al., Modified ZIF-8 nanoparticles attenuate osteoarthritis by reprogramming the metabolic pathway of synovial macrophages. *ACS Appl. Mater. Interfaces* **12**(2), 2009–2022 (2020). <https://doi.org/10.1021/acsami.9b16327>
174. M. He, L. Sun, X. Fu, S.P. McDonough, C.C. Chu, Biodegradable amino acid-based poly(ester amine) with tunable immunomodulating properties and their in vitro and in vivo wound healing studies in diabetic rats' wounds. *Acta Biomater.* **84**, 114–132 (2019). <https://doi.org/10.1016/j.actbio.2018.11.053>
175. X. Li, X. Wang, Q. Liu, J. Yan, D. Pan et al., ROS-responsive boronate-stabilized polyphenol-poloxamer 188 assembled dexamethasone nanodrug for macrophage repolarization in osteoarthritis treatment. *Adv. Healthc. Mater.* **10**(20), 2100883 (2021). <https://doi.org/10.1002/adhm.202100883>
176. L. Valls-Lacalle, I. Barba, E. Miro-Casas, J.J. Alburquerque-Bejar, M. Ruiz-Meana et al., Succinate dehydrogenase inhibition with malonate during reperfusion reduces infarct size by preventing mitochondrial permeability transition. *Cardiovasc. Res.* **109**(3), 374–384 (2016). <https://doi.org/10.1093/cvr/cvv279>
177. L. Davenport Huyer, S. Mandla, Y. Wang, S.B. Campbell, B. Yee et al., Macrophage immunomodulation through new polymers that recapitulate functional effects of itaconate as a power house of innate immunity. *Adv. Funct. Mater.* **31**(6), 2003341 (2020). <https://doi.org/10.1002/adfm.202003341>
178. J.R. Nakkala, Y. Yao, Z. Zhai, Y. Duan, D. Zhang et al., Dimethyl itaconate-loaded nanofibers rewrite macrophage polarization, reduce inflammation, and enhance repair of myocardial infarction. *Small* **17**(17), 2006992 (2021). <https://doi.org/10.1002/sml.202006992>
179. F. Zhu, L. Zi, P. Yang, Y. Wei, R. Zhong et al., Efficient iron and ROS nanoscavengers for brain protection after intracerebral hemorrhage. *ACS Appl. Mater. Interfaces* **13**(8), 9729–9738 (2021). <https://doi.org/10.1021/acsami.1c00491>
180. X. Dong, P. Wu, L. Yan, K. Liu, W. Wei et al., Oriented nanofibrous P(MMD-co-LA)/deferoxamine nerve scaffold facilitates peripheral nerve regeneration by regulating macrophage phenotype and revascularization. *Biomaterials* **280**, 121288 (2022). <https://doi.org/10.1016/j.biomaterials.2021.121288>
181. J. Han, Y.S. Kim, M.Y. Lim, H.Y. Kim, S. Kong et al., Dual roles of graphene oxide to attenuate inflammation and elicit timely polarization of macrophage phenotypes for cardiac repair. *ACS Nano* **12**(2), 1959–1977 (2018). <https://doi.org/10.1021/acsnano.7b09107>
182. Y. Li, X. Teng, C. Yang, Y. Wang, L. Wang et al., Ultrasound controlled anti-inflammatory polarization of platelet decorated microglia for targeted ischemic stroke therapy. *Angew. Chem. Int. Ed.* **60**(10), 5083–5090 (2021). <https://doi.org/10.1002/anie.202010391>
183. L. Chen, L. Zhang, H. Zhang, X. Sun, D. Liu et al., Programmable immune activating electrospun fibers for skin regeneration. *Bioactive. Mater.* **6**(10), 3218–3230 (2021). <https://doi.org/10.1016/j.bioactmat.2021.02.022>
184. T.T. Tang, B. Wang, M. Wu, Z.L. Li, Y. Feng et al., Extracellular vesicle-encapsulated IL-10 as novel nanotherapeutics against ischemic AKI. *Sci. Adv.* **6**(33), eaaz0748 (2020). <https://doi.org/10.1126/sciadv.aaz0748>
185. H. Kang, K. Zhang, D.S.H. Wong, F. Han, B. Li et al., Near-infrared light-controlled regulation of intracellular calcium to modulate macrophage polarization. *Biomaterials* **178**, 681–696 (2018). <https://doi.org/10.1016/j.biomaterials.2018.03.007>



186. X. Lei, G. Tan, Y. Wang, L. Chen, Y. Cao et al., Mitochondrial calcium nanoregulators reverse the macrophage pro-inflammatory phenotype through restoring mitochondrial calcium homeostasis for the treatment of osteoarthritis. *Int. J. Nanomedicine* **18**, 1469–1489 (2023). <https://doi.org/10.2147/IJN.S402170>
187. J. Wu, M. Wang, Y. Wu, J. Liu, W. Zhi et al., Coupling BCP ceramics with micro-vibration stimulation field for cascade amplification from immune activation to bone regeneration. *Adv. Funct. Mater.* **33**, 2215079 (2023). <https://doi.org/10.1002/adfm.202215079>
188. N. Feng, L. Liang, M. Fan, Y. Du, C. Chen et al., Treating autoimmune inflammatory diseases with an siERN1-nanoprodruge that mediates macrophage polarization and blocks Toll-like receptor signaling. *ACS Nano* **15**(10), 15874–15891 (2021). <https://doi.org/10.1021/acsnano.1c03726>
189. N. Li, Q. Du, Z. Jing, L. Xue, W. He et al., Study of the effects of Au@ZIF-8 on metabolism in mouse RAW 264.7 macrophages. *Biomater. Adv.* **138**, 212800 (2022). <https://doi.org/10.1016/j.bioadv.2022.212800>
190. H. Gu, Y. Zhu, J. Yang, R. Jiang, Y. Deng et al., Liver-inspired polyetherketoneketone scaffolds simulate regenerative signals and mobilize anti-inflammatory reserves to reprogram macrophage metabolism for boosted osteoporotic osseointegration. *Adv. Sci.* **10**(25), e2302136 (2023). <https://doi.org/10.1002/advs.202302136>
191. Y. Sang, Q. Deng, F. Cao, Z. Liu, Y. You et al., Remodeling macrophages by an iron nanotrapp for tumor growth suppression. *ACS Nano* **15**(12), 19298–19309 (2021). <https://doi.org/10.1021/acsnano.1c05392>
192. Y. Yang, Q. Tian, S. Wu, Y. Li, K. Yang et al., Blue light-triggered Fe<sup>2+</sup>-release from monodispersed ferrihydrite nanoparticles for cancer iron therapy. *Biomaterials* **271**, 120739 (2021). <https://doi.org/10.1016/j.biomaterials.2021.120739>
193. C.X. Li, Y. Zhang, X. Dong, L. Zhang, M.D. Liu et al., Artificially reprogrammed macrophages as tumor-tropic immunosuppression-resistant biologics to realize therapeutics production and immune activation. *Adv. Mater.* **31**(15), e1807211 (2019). <https://doi.org/10.1002/adma.201807211>
194. M.H. Oh, I.H. Sun, L. Zhao, R.D. Leone, I.M. Sun et al., Targeting glutamine metabolism enhances tumor-specific immunity by modulating suppressive myeloid cells. *J. Clin. Invest.* **130**(7), 3865–3884 (2020). <https://doi.org/10.1172/jci131859>
195. X.B. Shulan Han, Y. Zou, L. Wang, Y. Li, L. Yang et al., D-lactate modulates M2 tumor-associated macrophages and remodels immunosuppressive tumor microenvironment for hepatocellular carcinoma. *Sci. Adv.* **9**(29), eadg2697 (2023). <https://doi.org/10.1126/sciadv.adg2697>
196. J. Zhao, Z. Tian, S. Zhao, D. Feng, Z. Guo et al., Insights into the effect of catalytic intratumoral lactate depletion on metabolic reprogramming and immune activation for antitumoral activity. *Adv. Sci.* **10**(4), e2204808 (2023). <https://doi.org/10.1002/advs.202204808>
197. Z.Y. Han, C. Zhang, J.X. An, Y.Z. Wang, J.Y. Qiao et al., Metabolic regulation of tumor microenvironment with biohybrid bacterial bioreactor for enhanced cancer chemo-immunotherapy. *Adv. Funct. Mater.* **33**, 2302728 (2023). <https://doi.org/10.1002/adfm.202302728>
198. G.M. Tannahill, A.M. Curtis, J. Adamik, E.M. Palsson-McDermott, A.F. McGettrick et al., Succinate is an inflammatory signal that induces IL-1 $\beta$  through HIF-1 $\alpha$ . *Nature* **496**(7444), 238–242 (2013). <https://doi.org/10.1038/nature11986>
199. M.P. Murphy, L.A.J. O’Neill, Krebs cycle reimaged: The emerging roles of succinate and itaconate as signal transducers. *Cell* **174**(4), 780–784 (2018). <https://doi.org/10.1016/j.cell.2018.07.030>
200. E.T. Chouchani, V.R. Pell, E. Gaude, D. Aksentijevic, S.Y. Sundier et al., Ischaemic accumulation of succinate controls reperfusion injury through mitochondrial ROS. *Nature* **515**(7527), 431–435 (2014). <https://doi.org/10.1038/nature13909>
201. C.L. Strelko, W. Lu, F.J. Dufort, T.N. Seyfried, T.C. Chiles et al., Itaconic acid is a mammalian metabolite induced during macrophage activation. *J. Am. Chem. Soc.* **133**(41), 16386–16389 (2011). <https://doi.org/10.1021/ja2070889>
202. A. Michelucci, T. Cordes, J. Ghelfi, A. Pailot, N. Reiling et al., Immune-responsive gene 1 protein links metabolism to immunity by catalyzing itaconic acid production. *Proc. Natl. Acad. Sci. U.S.A.* **110**(19), 7820–7825 (2013). <https://doi.org/10.1073/pnas.1218599110>
203. W. Qin, K. Qin, Y. Zhang, W. Jia, Y. Chen et al., S-glycosylation-based cysteine profiling reveals regulation of glycolysis by itaconate. *Nat. Chem. Biol.* **15**(10), 983–991 (2019). <https://doi.org/10.1038/s41589-019-0323-5>
204. W. Qin, Y. Zhang, H. Tang, D. Liu, Y. Chen et al., Chemo-proteomic profiling of itaconation by bioorthogonal probes in inflammatory macrophages. *J. Am. Chem. Soc.* **142**(25), 10894–10898 (2020). <https://doi.org/10.1021/jacs.9b11962>
205. P. Sun, Z. Zhang, B. Wang, C. Liu, C. Chen et al., A genetically encoded fluorescent biosensor for detecting itaconate with subcellular resolution in living macrophages. *Nat. Commun.* **13**(1), 6562 (2022). <https://doi.org/10.1038/s41467-022-34306-5>
206. A. Hooftman, L.A.J. O’Neill, The immunomodulatory potential of the metabolite itaconate. *Trends Immunol.* **40**(8), 687–698 (2019). <https://doi.org/10.1016/j.it.2019.05.007>
207. V. Lampropoulou, A. Sergushichev, M. Bambouskova, S. Nair, E.E. Vincent et al., Itaconate links inhibition of succinate dehydrogenase with macrophage metabolic remodeling and regulation of inflammation. *Cell Metab.* **24**(1), 158–166 (2016). <https://doi.org/10.1016/j.cmet.2016.06.004>
208. L.A.J. O’Neill, M.N. Artyomov, Itaconate: the poster child of metabolic reprogramming in macrophage function. *Nat. Rev. Immunol.* **19**(5), 273–281 (2019). <https://doi.org/10.1038/s41577-019-0128-5>
209. E.L. Mills, D.G. Ryan, H.A. Prag, D. Dikovskaya, D. Menon et al., Itaconate is an anti-inflammatory metabolite that

- activates Nrf2 via alkylation of KEAP1. *Nature* **556**(7699), 113–117 (2018). <https://doi.org/10.1038/nature25986>
210. M. Bambouskova, L. Gorvel, V. Lampropoulou, A. Sergushichev, E. Loginicheva et al., Electrophilic properties of itaconate and derivatives regulate the Ikappabzeta-ATF3 inflammatory axis. *Nature* **556**(7702), 501–504 (2018). <https://doi.org/10.1038/s41586-018-0052-z>
211. L. Ni, Z. Lin, S. Hu, Y. Shi, Z. Jiang et al., Itaconate attenuates osteoarthritis by inhibiting STING/NF-kappaB axis in chondrocytes and promoting M2 polarization in macrophages. *Biochem. Pharmacol.* **198**, 114935 (2022). <https://doi.org/10.1016/j.bcp.2022.114935>
212. H. Yu, P. Ren, X. Pan, X. Zhang, J. Ma et al., Intracellular delivery of itaconate by metal-organic framework-anchored hydrogel microspheres for osteoarthritis therapy. *Pharmaceutics* **15**(3), 724 (2023). <https://doi.org/10.3390/pharmaceutics15030724>
213. Q. Ding, T. Sun, W. Su, X. Jing, B. Ye et al., Bioinspired multifunctional black phosphorus hydrogel with antibacterial and antioxidant properties: a stepwise countermeasure for diabetic skin wound healing. *Adv. Healthc. Mater.* **11**(12), e2102791 (2022). <https://doi.org/10.1002/adhm.202102791>
214. V.L. Nelson, H.C.B. Nguyen, J.C. Garcia-Canaveras, E.R. Briggs, W.Y. Ho et al., PPARgamma is a nexus controlling alternative activation of macrophages via glutamine metabolism. *Genes Dev.* **32**(15–16), 1035–1044 (2018). <https://doi.org/10.1101/gad.312355.118>
215. M.C. Runtsch, S. Angiari, A. Hoofman, R. Wadhwa, Y. Zhang et al., Itaconate and itaconate derivatives target JAK1 to suppress alternative activation of macrophages. *Cell Metab.* **34**(3), 487–50.e18 (2022). <https://doi.org/10.1016/j.cmet.2022.02.002>
216. V.C. Ganta, M.H. Choi, A. Kutateladze, T.E. Fox, C.R. Farber et al., A microRNA93-interferon regulatory factor-9-immunoresponsive gene-1-itaconic acid pathway modulates M2-like macrophage polarization to revascularize ischemic muscle. *Circulation* **135**(24), 2403–2425 (2017). <https://doi.org/10.1161/CIRCULATIONAHA.116.025490>
217. T. Ganz, E. Nemeth, Iron homeostasis in host defence and inflammation. *Nat. Rev. Immunol.* **15**(8), 500–510 (2015). <https://doi.org/10.1038/nri3863>
218. S. Recalcati, M. Locati, A. Marini, P. Santambrogio, F. Zaninotto et al., Differential regulation of iron homeostasis during human macrophage polarized activation. *Eur. J. Immunol.* **40**(3), 824–835 (2010). <https://doi.org/10.1002/eji.200939889>
219. C. Pfeifhofer-Obermair, P. Tymoszuk, V. Petzer, G. Weiss, M. Nairz, Iron in the tumor microenvironment-connecting the dots. *Front. Oncol.* **8**, 549 (2018). <https://doi.org/10.3389/fonc.2018.00549>
220. M. Jung, C. Mertens, B. Brune, Macrophage iron homeostasis and polarization in the context of cancer. *Immunobiology* **220**(2), 295–304 (2015). <https://doi.org/10.1016/j.imbio.2014.09.011>
221. S. Recalcati, M. Locati, E. Gammella, P. Invernizzi, G. Cairo, Iron levels in polarized macrophages: regulation of immunity and autoimmunity. *Autoimmun. Rev.* **11**(12), 883–889 (2012). <https://doi.org/10.1016/j.autrev.2012.03.003>
222. A.T. Aron, A.G. Reeves, C.J. Chang, Activity-based sensing fluorescent probes for iron in biological systems. *Curr. Opin. Chem. Biol.* **43**, 113–118 (2018). <https://doi.org/10.1016/j.cbpa.2017.12.010>
223. W. Xing, H. Xu, H. Ma, S.A.A. Abedi, S. Wang et al., A PET-based fluorescent probe for monitoring labile Fe(II) pools in macrophage activations and ferroptosis. *Chem. Commun.* **58**(18), 2979–2982 (2022). <https://doi.org/10.1039/d1cc06611k>
224. H.Y. Lin, R. Weissleder, E. Corradini, J.L. Babitt, Y. Xia et al., Method for measuring macrophage iron efflux in vitro and in vivo using magnetic resonance imaging. *Blood* **112**(11), 4636–4636 (2008). <https://doi.org/10.1182/blood.V112.11.4636.4636>
225. A. Leftin, N. Ben-Chetrit, J.A. Joyce, J.A. Koutcher, Imaging endogenous macrophage iron deposits reveals a metabolic biomarker of polarized tumor macrophage infiltration and response to CSF1R breast cancer immunotherapy. *Sci. Rep.* **9**(1), 857 (2019). <https://doi.org/10.1038/s41598-018-37408-7>
226. A. Biesemeier, O. Eibl, S. Eswara, J.N. Audinot, T. Wirtz et al., Transition metals and trace elements in the retinal pigment epithelium and choroid: correlative ultrastructural and chemical analysis by analytical electron microscopy and nano-secondary ion mass spectrometry. *Metallomics* **10**(2), 296–308 (2018). <https://doi.org/10.1039/c7mt00259a>
227. F. Penen, J. Malherbe, M.P. Isaure, D. Dobritzsch, I. Bertalan et al., Chemical bioimaging for the subcellular localization of trace elements by high contrast TEM, TEM/X-EDS, and NanoSIMS. *J. Trace Elem. Med. Biol.* **37**, 62–68 (2016). <https://doi.org/10.1016/j.jtemb.2016.04.014>
228. J. Lovric, N. Najafinobar, M.E. Kurczyk, O. De Castro, A. Biesemeier et al., Correlative high-resolution imaging of iron uptake in lung macrophages. *Anal. Chem.* **94**(37), 12798–12806 (2022). <https://doi.org/10.1021/acs.analchem.2c02675>
229. Y. Zhou, K.T. Que, Z. Zhang, Z.J. Yi, P.X. Zhao et al., Iron overloaded polarizes macrophage to proinflammation phenotype through ROS/acetyl-p53 pathway. *Cancer Med.* **7**(8), 4012–4022 (2018). <https://doi.org/10.1002/cam4.1670>
230. H. She, S. Xiong, M. Lin, E. Zandi, C. Giulivi et al., Iron activates NF-kappaB in kupffer cells. *Am. J. Physiol. Gastrointest. Liver Physiol.* **283**(3), G719–726 (2002). <https://doi.org/10.1152/ajpgi.00108.2002>
231. P. Handa, S. Thomas, V. Morgan-Stevenson, B.D. Maliken, E. Gochanour et al., Iron alters macrophage polarization status and leads to steatohepatitis and fibrogenesis. *J. Leukoc. Biol.* **105**(5), 1015–1026 (2019). <https://doi.org/10.1002/JLB.3A0318-108R>
232. H. Kim, J.Y. Hong, W.J. Jeon, J. Lee, Y.J. Lee et al., Melittin regulates iron homeostasis and mediates macrophage polarization in rats with lumbar spinal stenosis. *Biomed. Pharmacother.* **156**, 113776 (2022). <https://doi.org/10.1016/j.biopha.2022.113776>



233. E. Patino, D. Bhatia, S.Z. Vance, A. Antypiuk, R. Uni et al., Iron therapy mitigates chronic kidney disease progression by regulating intracellular iron status of kidney macrophages. *JCI Insight* **8**(1), e159235 (2023). <https://doi.org/10.1172/jci.insight.159235>
234. D.G. DeNardo, B. Ruffell, Macrophages as regulators of tumour immunity and immunotherapy. *Nat. Rev. Immunol.* **19**(6), 369–382 (2019). <https://doi.org/10.1038/s41577-019-0127-6>
235. H. Zhao, R. Liu, L. Wang, F. Tang, W. Chen et al., Artificial macrophage with hierarchical nanostructure for biomimetic reconstruction of antitumor immunity. *Nano-Micro Lett.* **15**(1), 216 (2023). <https://doi.org/10.1007/s40820-023-01193-4>
236. S. Zanganeh, G. Hutter, R. Spitler, O. Lenkov, M. Mahmoudi et al., Iron oxide nanoparticles inhibit tumour growth by inducing pro-inflammatory macrophage polarization in tumour tissues. *Nat. Nanotechnol.* **11**(11), 986–994 (2016). <https://doi.org/10.1038/nnano.2016.168>
237. Z. Liu, W. Jiang, J. Nam, J.J. Moon, B.Y.S. Kim, Immunomodulating nanomedicine for cancer therapy. *Nano Lett.* **18**(11), 6655–6659 (2018). <https://doi.org/10.1021/acs.nanolett.8b02340>
238. Z. Liu, J. Qiao, T. Nagy, M.P. Xiong, ROS-triggered degradable iron-chelating nanogels: safely improving iron elimination in vivo. *J. Control. Release* **283**, 84–93 (2018). <https://doi.org/10.1016/j.jconrel.2018.05.025>
239. R. Agoro, M. Taleb, V.F.J. Quesniaux, C. Mura, Cell iron status influences macrophage polarization. *PLoS ONE* **13**(5), e0196921 (2018). <https://doi.org/10.1371/journal.pone.0196921>
240. H.N. Wilkinson, E.R. Roberts, A.R. Stafford, K.L. Banyard, P. Matteucci et al., Tissue iron promotes wound repair via M2 macrophage polarization and the chemokine (C-C Motif) ligands 17 and 22. *Am. J. Pathol.* **189**(11), 2196–2208 (2019). <https://doi.org/10.1016/j.ajpath.2019.07.015>
241. Z.S. Gan, Q.Q. Wang, J.H. Li, X.L. Wang, Y.Z. Wang et al., Iron reduces M1 macrophage polarization in RAW264.7 macrophages associated with inhibition of STAT1. *Mediators Inflamm.* **2017**, 8570818 (2017). <https://doi.org/10.1155/2017/8570818>
242. D. Li, C. Beisswenger, C. Herr, R.M. Schmid, R.L. Gallo et al., Expression of the antimicrobial peptide cathelicidin in myeloid cells is required for lung tumor growth. *Oncogene* **33**(21), 2709–2716 (2014). <https://doi.org/10.1038/onc.2013.248>
243. X. Zhou, W. Yang, J. Li, Ca<sup>2+</sup>- and protein kinase C-dependent signaling pathway for nuclear factor-kappaB activation, inducible nitric-oxide synthase expression, and tumor necrosis factor-alpha production in lipopolysaccharide-stimulated rat peritoneal macrophages. *J. Biol. Chem.* **281**(42), 31337–31347 (2006). <https://doi.org/10.1074/jbc.M602739200>
244. E.Y. Moon, S. Pyo, Lipopolysaccharide stimulates Epac1-mediated Rap1/NF-kappaB pathway in Raw 264.7 murine macrophages. *Immunol. Lett.* **110**(2), 121–125 (2007). <https://doi.org/10.1016/j.imlet.2007.04.002>
245. L.C. Denlinger, P.L. Fiset, K.A. Garis, G. Kwon, A. Vazquez-Torres et al., Regulation of inducible nitric oxide synthase expression by macrophage purinoreceptors and calcium. *J. Biol. Chem.* **271**(1), 337–342 (1996). <https://doi.org/10.1074/jbc.271.1.337>
246. Y. Ye, X. Huang, Y. Zhang, X. Lai, X. Wu et al., Calcium influx blocked by SK&K 96365 modulates the LPS plus IFN-gamma-induced inflammatory response in murine peritoneal macrophages. *Int. Immunopharmacol.* **12**(2), 384–393 (2012). <https://doi.org/10.1016/j.intimp.2011.12.011>
247. S.Y. Ji, H. Lee, H. Hwangbo, S.H. Hong, H.J. Cha et al., A novel peptide oligomer of bacitracin induces M1 macrophage polarization by facilitating Ca<sup>2+</sup> influx. *Nutrients* **12**(6), 1603 (2020). <https://doi.org/10.3390/nu12061603>
248. J. Mo, Y. Xu, X. Wang, W. Wei, J. Zhao, Exploiting the protein corona: coating of black phosphorus nanosheets enables macrophage polarization via calcium influx. *Nanoscale* **12**(3), 1742–1748 (2020). <https://doi.org/10.1039/c9nr08570j>
249. A. Chauhan, Y. Sun, P. Sukumaran, F.O. Quenum Zangbede, C.N. Jondle et al., M1 macrophage polarization is dependent on TRPC1-mediated calcium entry. *iScience* **8**, 85–102 (2018). <https://doi.org/10.1016/j.isci.2018.09.014>
250. Z. Yin, T. Ma, Y. Lin, X. Lu, C. Zhang et al., IL-6/STAT3 pathway intermediates M1/M2 macrophage polarization during the development of hepatocellular carcinoma. *J. Cell. Biochem.* **119**(11), 9419–9432 (2018). <https://doi.org/10.1002/jcb.27259>
251. N. Ding, Y. Wang, C. Dou, F. Liu, G. Guan et al., Physalin D regulates macrophage M1/M2 polarization via the STAT1/6 pathway. *J. Cell. Physiol.* **234**(6), 8788–8796 (2019). <https://doi.org/10.1002/jcp.27537>
252. H. Jiang, M.B. Harris, P. Rothman, IL-4/IL-13 signaling beyond JAK/STAT. *J. Allergy Clin. Immunol.* **105**(6 Pt 1), 1063–1070 (2000). <https://doi.org/10.1067/mai.2000.107604>
253. G. Nappo, F. Handle, F.R. Santer, R.V. McNeill, R.I. Seed et al., The immunosuppressive cytokine interleukin-4 increases the clonogenic potential of prostate stem-like cells by activation of STAT6 signalling. *Oncogenesis* **6**(5), e342 (2017). <https://doi.org/10.1038/oncsis.2017.23>
254. S. Su, Q. Zhao, C. He, D. Huang, J. Liu et al., miR-142-5p and miR-130a-3p are regulated by IL-4 and IL-13 and control profibrogenic macrophage program. *Nat. Commun.* **6**, 8523 (2015). <https://doi.org/10.1038/ncomms9523>
255. F.O. Martinez, L. Helming, R. Milde, A. Varin, B.N. Melgert et al., Genetic programs expressed in resting and IL-4 alternatively activated mouse and human macrophages: similarities and differences. *Blood* **121**(9), e57–69 (2013). <https://doi.org/10.1182/blood-2012-06-436212>
256. P.J. Murray, J.E. Allen, S.K. Biswas, E.A. Fisher, D.W. Gilroy et al., Macrophage activation and polarization: nomenclature and experimental guidelines. *Immunity* **41**(1), 14–20 (2014). <https://doi.org/10.1016/j.immuni.2014.06.008>
257. K. Nelms, A.D. Keegan, J. Zamorano, J.J. Ryan, W.E. Paul, The IL-4 receptor: signaling mechanisms and biologic

- functions. *Annu. Rev. Immunol.* **17**, 701–738 (1999). <https://doi.org/10.1146/annurev.immunol.17.1.701>
258. S.C. Huang, A.M. Smith, B. Everts, M. Colonna, E.L. Pearce et al., Metabolic reprogramming mediated by the mTORC2-IRF4 signaling axis is essential for macrophage alternative activation. *Immunity* **45**(4), 817–830 (2016). <https://doi.org/10.1016/j.immuni.2016.09.016>
259. A.S. Divakaruni, W.Y. Hsieh, L. Minarrieta, T.N. Duong, K.K.O. Kim et al., Etomoxir inhibits macrophage polarization by disrupting CoA homeostasis. *Cell Metab.* **28**(3), 490–50.e37 (2018). <https://doi.org/10.1016/j.cmet.2018.06.001>
260. J. Lundin, E. Kimby, L. Bergmann, T. Karakas, H. Mellstedt et al., Interleukin 4 therapy for patients with chronic lymphocytic leukaemia: a phase I/II study. *Br. J. Haematol.* **112**(1), 155–160 (2001). <https://doi.org/10.1046/j.1365-2141.2001.02525.x>
261. Y. Qian, L. Li, Y. Song, L. Dong, P. Chen et al., Surface modification of nanofibrous matrices via layer-by-layer functionalized silk assembly for mitigating the foreign body reaction. *Biomaterials* **164**, 22–37 (2018). <https://doi.org/10.1016/j.biomaterials.2018.02.038>
262. X. Ge, J. Hu, Y. Peng, Z. Zeng, D. He et al., Atmosphere-inspired multilayered nanoarmor with modulable protection and delivery of interleukin-4 for inflammatory microenvironment modulation. *Biomaterials* **301**, 122254 (2023). <https://doi.org/10.1016/j.biomaterials.2023.122254>
263. V. Spieler, M.G. Ludwig, J. Dawson, B. Tigani, A. Littlewood-Evans et al., Targeting interleukin-4 to the arthritic joint. *J. Control. Release* **326**, 172–180 (2020). <https://doi.org/10.1016/j.jconrel.2020.07.005>
264. R. Lang, D. Patel, J.J. Morris, R.L. Rutschman, P.J. Murray, Shaping gene expression in activated and resting primary macrophages by IL-10. *J. Immunol.* **169**(5), 2253–2263 (2002). <https://doi.org/10.4049/jimmunol.169.5.2253>
265. P.J. Murray, The primary mechanism of the IL-10-regulated antiinflammatory response is to selectively inhibit transcription. *Proc. Natl. Acad. Sci. U.S.A.* **102**(24), 8686–8691 (2005). <https://doi.org/10.1073/pnas.0500419102>
266. W. Ouyang, S. Rutz, N.K. Crellin, P.A. Valdez, S.G. Hymowitz, Regulation and functions of the IL-10 family of cytokines in inflammation and disease. *Annu. Rev. Immunol.* **29**, 71–109 (2011). <https://doi.org/10.1146/annurev-immunol-031210-101312>
267. J. Patel, IL-10 reprogramming of metabolism in macrophages through mitophagy. *Cardiovasc. Res.* **113**(11), e40–e41 (2017). <https://doi.org/10.1093/cvr/cvx144>
268. K. Minton, Immune regulation: IL-10 targets macrophage metabolism. *Nat. Rev. Immunol.* **17**(6), 345 (2017). <https://doi.org/10.1038/nri.2017.57>
269. C.J. Huang, B.R. Stevens, R.B. Nielsen, P.N. Slovin, X. Fang et al., Interleukin-10 inhibition of nitric oxide biosynthesis involves suppression of CAT-2 transcription. *Nitric Oxide* **6**(1), 79–84 (2002). <https://doi.org/10.1006/niox.2001.0402>
270. W.C. Huang, Y.S. Lin, C.Y. Wang, C.C. Tsai, H.C. Tseng et al., Glycogen synthase kinase-3 negatively regulates anti-inflammatory interleukin-10 for lipopolysaccharide-induced iNOS/NO biosynthesis and RANTES production in microglial cells. *Immunology* **128**(1 Suppl), e275–286 (2009). <https://doi.org/10.1111/j.1365-2567.2008.02959.x>
271. T. Schreiber, S. Ehlers, L. Heitmann, A. Rausch, J. Mages et al., Autocrine IL-10 induces hallmarks of alternative activation in macrophages and suppresses antituberculosis effector mechanisms without compromising T cell immunity. *J. Immunol.* **183**(2), 1301–1312 (2009). <https://doi.org/10.4049/jimmunol.0803567>
272. M. Jung, Y. Ma, R.P. Iyer, K.Y. DeLeon-Pennell, A. Yabluchanskiy et al., IL-10 improves cardiac remodeling after myocardial infarction by stimulating M2 macrophage polarization and fibroblast activation. *Basic Res. Cardiol.* **112**(3), 33 (2017). <https://doi.org/10.1007/s00395-017-0622-5>
273. O.P.B. Wiklander, M.A. Brennan, J. Lotvall, X.O. Breakefield, S. El Andaloussi, Advances in therapeutic applications of extracellular vesicles. *Sci. Transl. Med.* **11**(492), eaav8521 (2019). <https://doi.org/10.1126/scitranslmed.aav8521>
274. D. Li, K. Chen, H. Tang, S. Hu, L. Xin et al., A logic-based diagnostic and therapeutic hydrogel with multi-stimuli responsiveness to orchestrate diabetic bone regeneration. *Adv. Mater.* **34**(11), e2108430 (2021). <https://doi.org/10.1002/adma.202108430>
275. R. Stienstra, R.T. Netea-Maier, N.P. Riksen, L.A.B. Joosten, M.G. Netea, Specific and complex reprogramming of cellular metabolism in myeloid cells during innate immune responses. *Cell Metab.* **26**(1), 142–156 (2017). <https://doi.org/10.1016/j.cmet.2017.06.001>
276. M. Munder, K. Eichmann, M. Modolell, Alternative metabolic states in murine macrophages reflected by the nitric oxide synthase/arginase balance: competitive regulation by CD4+ T cells correlates with Th1/Th2 phenotype. *J. Immunol.* **160**(11), 5347–5354 (1998). <https://doi.org/10.4049/jimmunol.160.11.5347>
277. N. Hannemann, S. Cao, D. Eriksson, A. Schnelzer, J. Jordan et al., Transcription factor Fra-1 targets arginase-1 to enhance macrophage-mediated inflammation in arthritis. *J. Clin. Invest.* **129**(7), 2669–2684 (2019). <https://doi.org/10.1172/JCI96832>
278. J.K. Dowling, R. Afzal, L.J. Gearing, M.P. Cervantes-Silva, S. Annett et al., Mitochondrial arginase-2 is essential for IL-10 metabolic reprogramming of inflammatory macrophages. *Nat. Commun.* **12**(1), 1460 (2021). <https://doi.org/10.1038/s41467-021-21617-2>
279. C. De Santi, F.K. Nally, R. Afzal, C.P. Duffy, S. Fitzsimons et al., Enhancing arginase 2 expression using target site blockers as a strategy to modulate macrophage phenotype. *Mol. Ther. Nucleic Acids* **29**, 643–655 (2022). <https://doi.org/10.1016/j.omtn.2022.08.004>
280. Y. Mao, D. Shi, G. Li, P. Jiang, Citrulline depletion by ASS1 is required for proinflammatory macrophage activation and immune responses. *Mol. Cell* **82**(3), 527–541.e527 (2022). <https://doi.org/10.1016/j.molcel.2021.12.006>
281. M. Kieler, M. Hofmann, G. Schabbauer, More than just protein building blocks: How amino acids and related

- metabolic pathways fuel macrophage polarization. *FEBS J.* **288**(12), 3694–3714 (2021). <https://doi.org/10.1111/febs.15715>
282. W. Ren, Y. Xia, S. Chen, G. Wu, F.W. Bazer et al., Glutamine metabolism in macrophages: a novel target for obesity/type 2 diabetes. *Adv. Nutr.* **10**(2), 321–330 (2019). <https://doi.org/10.1093/advances/nmy084>
283. P.S. Liu, H. Wang, X. Li, T. Chao, T. Teav et al., Alpha-ketoglutarate orchestrates macrophage activation through metabolic and epigenetic reprogramming. *Nat. Immunol.* **18**(9), 985–994 (2017). <https://doi.org/10.1038/ni.3796>
284. M.H. Pai, C.S. Lei, S.T. Su, S.L. Yeh, Y.C. Hou, Effects of dietary glutamine supplementation on immune cell polarization and muscle regeneration in diabetic mice with limb ischemia. *Eur. J. Nutr.* **59**(3), 921–933 (2020). <https://doi.org/10.1007/s00394-019-01951-4>
285. E.M. Palmieri, A. Menga, R. Martin-Perez, A. Quinto, C. Riera-Domingo et al., Pharmacologic or genetic targeting of glutamine synthetase skews macrophages toward an M1-like phenotype and inhibits tumor metastasis. *Cell Rep.* **20**(7), 1654–1666 (2017). <https://doi.org/10.1016/j.celrep.2017.07.054>
286. X. Shan, P. Hu, L. Ni, L. Shen, Y. Zhang et al., Serine metabolism orchestrates macrophage polarization by regulating the IGF1-p38 axis. *Cell. Mol. Immunol.* **19**(11), 1263–1278 (2022). <https://doi.org/10.1038/s41423-022-00925-7>
287. A.E. Rodriguez, G.S. Ducker, L.K. Billingham, C.A. Martinez, N. Mainolfi et al., Serine metabolism supports macrophage IL-1 $\beta$  production. *Cell Metab.* **29**(4), 1003–101.e14 (2019). <https://doi.org/10.1016/j.cmet.2019.01.014>
288. R. Haas, D. Cucchi, J. Smith, V. Pucino, C.E. Macdougall et al., Intermediates of metabolism: from bystanders to signalling molecules. *Trends Biochem. Sci.* **41**(5), 460–471 (2016). <https://doi.org/10.1016/j.tibs.2016.02.003>
289. U.E. Martinez-Outschoorn, M. Prisco, A. Ertel, A. Tsirigos, Z. Lin et al., Ketones and lactate increase cancer cell “stemness,” driving recurrence, metastasis and poor clinical outcome in breast cancer: achieving personalized medicine via metabolo-genomics. *Cell Cycle* **10**(8), 1271–1286 (2011). <https://doi.org/10.4161/cc.10.8.15330>
290. S.E.A. Selleri, Human mesenchymal stromal cell-secreted lactate induces M2-macrophage differentiation by metabolic reprogramming. *Oncotarget* **7**(21), 30193–30210 (2016). <https://doi.org/10.18632/oncotarget.8623>
291. R.D. Leone, J.D. Powell, Metabolism of immune cells in cancer. *Nat. Rev. Cancer* **20**(9), 516–531 (2020). <https://doi.org/10.1038/s41568-020-0273-y>
292. D. O’Sullivan, D.E. Sanin, E.J. Pearce, E.L. Pearce, Metabolic interventions in the immune response to cancer. *Nat. Rev. Immunol.* **19**(5), 324–335 (2019). <https://doi.org/10.1038/s41577-019-0140-9>
293. O.R. Colegio, N.Q. Chu, A.L. Szabo, T. Chu, A.M. Rhebergen et al., Functional polarization of tumour-associated macrophages by tumour-derived lactic acid. *Nature* **513**(7519), 559–563 (2014). <https://doi.org/10.1038/nature13490>
294. D. Zhang, Z. Tang, H. Huang, G. Zhou, C. Cui et al., Metabolic regulation of gene expression by histone lactylation. *Nature* **574**(7779), 575–580 (2019). <https://doi.org/10.1038/s41586-019-1678-1>
295. B. McDonald, A.Z. Zucoloto, I.-L. Yu, R. Burkhard, K. Brown et al., Programming of an intravascular immune firewall by the gut microbiota protects against pathogen dissemination during infection. *Cell Host Microbe* **28**(5), 660–668.e4 (2020). <https://doi.org/10.1016/j.chom.2020.07.014>
296. T. Takeuchi, S. Matile, Sensing applications of synthetic transport systems. *Chem. Commun.* **49**(1), 19–29 (2013). <https://doi.org/10.1039/c2cc36729g>
297. H. Wang, C. Wu, X. Tong, S. Chen, A biomimetic metal-organic framework nanosystem modulates immunosuppressive tumor microenvironment metabolism to amplify immunotherapy. *J. Control. Release* **353**, 727–737 (2023). <https://doi.org/10.1016/j.jconrel.2022.11.054>
298. Z.X. Liao, Y.C. Fa, I.M. Kempson, S.J. Tseng, Repolarization of M2 to M1 macrophages triggered by lactate oxidase released from methylcellulose hydrogel. *Bioconjug. Chem.* **30**(10), 2697–2702 (2019). <https://doi.org/10.1021/acs.biocconjchem.9b00618>
299. Y.F. Lu, H.S. Li, J. Wang, M.Y. Yao, Y. Peng et al., Engineering bacteria-activated multifunctionalized hydrogel for promoting diabetic wound healing. *Adv. Funct. Mater.* **31**(48), 210574 (2021). <https://doi.org/10.1002/adfm.202105749>
300. E. Blanco, H. Shen, M. Ferrari, Principles of nanoparticle design for overcoming biological barriers to drug delivery. *Nat. Biotechnol.* **33**(9), 941–951 (2015). <https://doi.org/10.1038/nbt.3330>
301. Y. Yang, L. Guo, Z. Wang, P. Liu, X. Liu et al., Targeted silver nanoparticles for rheumatoid arthritis therapy via macrophage apoptosis and re-polarization. *Biomaterials* **264**, 120390 (2021). <https://doi.org/10.1016/j.biomaterials.2020.120390>
302. F. Wang, L. Wen, J. Liu, W. Peng, Z. Meng et al., Albumin nanocomposites with MnO<sub>2</sub>/Gd<sub>2</sub>O<sub>3</sub> motifs for precise mr imaging of acute myocardial infarction in rabbit models. *Biomaterials* **230**, 119614 (2020). <https://doi.org/10.1016/j.biomaterials.2019.119614>
303. A. Hoofman, C.G. Peace, D.G. Ryan, E.A. Day, M. Yang et al., Macrophage fumarate hydratase restrains mtRNA-mediated interferon production. *Nature* **615**(7952), 490–498 (2023). <https://doi.org/10.1038/s41586-023-05720-6>
304. S. Yeudall, C.M. Upchurch, P.V. Seegren, C.M. Pavelec, J. Greulich et al., Macrophage acetyl-CoA carboxylase regulates acute inflammation through control of glucose and lipid metabolism. *Sci. Adv.* **8**(47), eadq1984 (2022). <https://doi.org/10.1126/sciadv.abq1984>
305. J. Ma, K. Wei, J. Liu, K. Tang, H. Zhang et al., Glycogen metabolism regulates macrophage-mediated acute inflammatory responses. *Nat. Commun.* **11**(1), 1769 (2020). <https://doi.org/10.1038/s41467-020-15636-8>
306. Y. Dong, J. Zhang, Y. Wang, Y. Zhang, D. Rappaport et al., Intracavitary spraying of nanoregulator-encased hydrogel modulates cholesterol metabolism of glioma-supportive

- macrophage for postoperative glioblastoma immunotherapy. *Adv. Mater.* **36**(13), e2311109 (2024). <https://doi.org/10.1002/adma.202311109>
307. A.C. Thomas, J.T. Mattila, “Of mice and men”: arginine metabolism in macrophages. *Front. Immunol.* **5**, 479 (2014). <https://doi.org/10.3389/fimmu.2014.00479>
308. J.B. Weinberg, M.A. Misukonis, P.J. Shami, S.N. Mason, D.L. Sauls et al., Human mononuclear phagocyte inducible nitric oxide synthase (iNOS): analysis of iNOS mRNA, iNOS protein, bioppterin, and nitric oxide production by blood monocytes and peritoneal macrophages. *Blood* **86**(3), 1184–1195 (1995). <https://doi.org/10.1182/blood.V86.3.1184.1184>
309. S.J. Jackson, G.J. Thomas, Human tissue models in cancer research: Looking beyond the mouse. *Dis. Model. Mech.* **10**(8), 939–942 (2017). <https://doi.org/10.1242/dmm.031260>
310. M. Fujii, M. Shimokawa, S. Date, A. Takano, M. Matano et al., A colorectal tumor organoid library demonstrates progressive loss of niche factor requirements during tumorigenesis. *Cell Stem Cell* **18**(6), 827–838 (2016). <https://doi.org/10.1016/j.stem.2016.04.003>
311. D.K. Zhao, J. Liang, X.Y. Huang, S. Shen, J. Wang, Organoids technology for advancing the clinical translation of cancer nanomedicine. *Wiley Interdiscip. Rev. Nanomed. Nanobiotechnol.* **15**(5), e1892 (2023). <https://doi.org/10.1002/wnan.1892>
312. M. Faria, M. Björnmalm, K.J. Thurecht, S.J. Kent, R.G. Parton et al., Minimum information reporting in bio-nano experimental literature. *Nat. Nanotechnol.* **13**(9), 777–785 (2018). <https://doi.org/10.1038/s41565-018-0246-4>
313. O. Adir, M. Poley, G. Chen, S. Froim, N. Krinsky et al., Integrating artificial intelligence and nanotechnology for precision cancer medicine. *Adv. Mater.* **32**(13), e1901989 (2020). <https://doi.org/10.1002/adma.201901989>
314. Y. Wang, S. Sun, Z. Zhang, D. Shi, Nanomaterials for cancer precision medicine. *Adv. Mater.* **30**(17), e1705660 (2018). <https://doi.org/10.1002/adma.201705660>
315. J.I. Joo, M. Choi, S.H. Jang, S. Choi, S.M. Park et al., Realizing cancer precision medicine by integrating systems biology and nanomaterial engineering. *Adv. Mater.* **32**(35), e1906783 (2020). <https://doi.org/10.1002/adma.201906783>

